Charmless two-body $B_{(s)} \to VP$ decays in soft collinear effective theory

Wei Wang,[1,2] Yu-Ming Wang,[1,2] De-Shan Yang,[2] and Cai-Dian Lü[1]

[1]*Institute of High Energy Physics, Chinese Academy of Sciences, Beijing 100049, People's Republic of China*
[2]*Graduate University of Chinese Academy of Sciences, Beijing 100049, People's Republic of China*

(Received 2 April 2008; published 13 August 2008)

We provide the analysis of charmless two-body $B \to VP$ decays under the framework of the soft collinear effective theory (SCET), where $V(P)$ denotes a light vector (pseudoscalar) meson. Besides the leading power contributions, some power corrections (chiraly enhanced penguins) are also taken into account. Using the current available $B \to PP$ and $B \to VP$ experimental data on branching fractions and CP asymmetry variables, we find two kinds of solutions in χ^2 fit for the 16 nonperturbative inputs which are essential in the 87 $B \to PP$ and $B \to VP$ decay channels. Chiraly enhanced penguins can change several charming penguins sizably, since they share the same topology. However, most of the other nonperturbative inputs and predictions on branching ratios and CP asymmetries are not changed too much. With the two sets of inputs, we predict the branching fractions and CP asymmetries of other modes especially $B_s \to VP$ decays. The agreements and differences with results in QCD factorization and perturbative QCD approach are analyzed. We also study the time-dependent CP asymmetries in channels with CP eigenstates in the final states and some other channels such as $\bar{B}^0/B^0 \to \pi^{\pm}\rho^{\mp}$ and $\bar{B}_s^0/B_s^0 \to K^{\pm}K^{*\mp}$. In the perturbative QCD approach, the $(S-P)(S+P)$ penguins in annihilation diagrams play an important role. Although they have the same topology with charming penguins in SCET, there are many differences between the two objects in weak phases, magnitudes, strong phases, and factorization properties.

DOI: 10.1103/PhysRevD.78.034011 PACS numbers: 13.25.Hw, 14.65.Fy, 12.39.Hg

I. INTRODUCTION

Studies on B decays are mainly concentrated on the precise test of the standard model (SM) and the search for possible new physics scenarios. To map out the apex in the unitarity triangle of the Cabibbo-Kobayashi-Maskawa (CKM) matrix, many precise experimental data together with reliable theoretical predictions are required. In charmless two-body nonleptonic B decays, the main experimental observables are branching ratios and CP asymmetries. To predict these observables, one has to compute the hadronic decay amplitudes $\langle M_1 M_2|O_i|B\rangle$, where O_i is typically a four-quark or a magnetic moment type operator. Since three hadronic states are involved in these decays, the predictions on these observables are often polluted by our poor knowledge of the nonperturbative QCD. Fortunately, it has been suggested that in the $m_b \to \infty$ limit, decay amplitudes can be studied in a well-organized way: they can be factorized into the convolution of nonperturbative objects such as B to light form factors and decay constants of light pseudoscalars/vectors with perturbative hard kernels. In recent years, great progresses have been made in studies of charmless two-body B decays. These decays were investigated in the so-called naive factorization approach [1,2] and the generalized factorization approach [3–7]. At present, there are three commonly accepted theoretical approaches to investigate the dynamics of these decays, the QCD factorization (QCDF) [8–10], the perturbative QCD (PQCD) [11–13], and the soft collinear effective theory (SCET) [14,15]. Despite many differences, all of them are based on power expansions in $\Lambda_{\rm QCD}/m_b$, where m_b is the b-quark mass and $\Lambda_{\rm QCD}$ is the typical hadronic scale. Factorization of the hadronic matrix elements is proved to hold in the leading power in $\Lambda_{\rm QCD}/m_b$ in a number of decays.

In the present work, we will focus on the SCET. The matching from QCD onto SCET is always performed in two stages. The fluctuations with off-shellness $\mathcal{O}(m_b^2)$ is first integrated out and one results in the intermediate effective theory. At the final stage, we integrate out the hard-collinear modes with off-shellness $\mathcal{O}(m_b\Lambda_{\rm QCD})$ to derive SCET$_{\rm II}$. In $B \to M_1 M_2$ decays, both of the final state mesons move very fast and are generated back-to-back in the rest frame of the B meson. Correspondingly, there exist three typical scales: the b quark mass m_b, the soft scale $\Lambda_{\rm QCD}$ set by the typical momentum of the light degrees of freedom in the heavy B meson, and the intermediate scale $\sqrt{m_b\Lambda_{\rm QCD}}$ which arises from the interaction between collinear particles and soft modes. SCET provides an elegant theoretical tool to separate the physics at different scales and factorization for $B \to M_1 M_2$ proved to hold to all orders in α_s at leading power of $1/m_b$ [16–20]. After integrating out the fluctuations with off-shellness m_b^2, one reaches the intermediate effective theory SCET$_{\rm I}$, in which the generic factorization formula for $B \to M_1 M_2$ is written

by

$$\langle M_1M_2|O_i|B\rangle = T(u) \otimes \phi_{M_1}(u)\zeta^{B\to M_2} + T_J(u,z) \otimes \phi_{M_1}(u) \otimes \zeta_J^{B\to M_2}(z), \quad (1)$$

where T and T_J are perturbatively calculable Wilson coefficients which depend on the Lorentz structure and flavor structure. Calculations for these hard kernel functions are approaching next-to-leading order accuracy [8,9,19,21–23]. In the second step, the fluctuations with typical off-shellness $m_b\Lambda_{\rm QCD}$ are integrated out and one reaches $\rm SCET_{II}$. In $\rm SCET_{II}$, end-point singularities prohibit the factorization of ζ, while the function ζ_J can be further factorized into the convolution of a hard kernel (jet function) with light-cone distribution amplitudes:

$$\zeta_J(z) = \phi_{M_2}(x) \otimes J(z,x,k_+) \otimes \phi_B(k_+). \quad (2)$$

An essential question is whether power corrections in SCET can be analyzed in a similar way. It is almost an impossible task to include all power corrections, but we can include the relatively important one. Importance of chiraly enhanced penguins was noted a long time ago, and numerics show that chirally enhanced penguins are comparable with the penguin contributions at leading power. Thus in both of QCDF [8–10] and PQCD [11–13] approaches, it has been incorporated into the decay amplitudes besides the leading power penguins. In SCET, the complete operator basis and the corresponding factorization formulas for this term are recently derived in Refs. [23,24]. A new factorization formula for chirally enhanced penguin was proved to hold to all orders in α_s, and more importantly the factorization formula does not suffer from the end-point divergence. In the factorization formula, a new form factor named ζ_χ and a twist-3 light-cone distribution amplitude ϕ^{pp} are introduced.

In Ref. [25], one phenomenological framework is introduced, in which the expansion at the intermediate scale $\mu_{hc} = \sqrt{m_b\Lambda_{\rm QCD}}$ is not used. Instead the experimental data are used to fit the nonperturbative inputs. This method is very useful especially at tree level, since the function $T(u)$ is a constant and $T_J(u,z)$ is a function of only u. Thus only a few inputs are required in decay amplitudes. In this framework, an additional term from the intermediate charm quark loops, which is called charming penguin [20,25–29], is also taken into account. Charming penguins are not factorized into the LCDAs and form factors, since the heavy charm quark pair cannot be viewed as collinear quarks. They are also treated as nonperturbative inputs. This method is first applied to $B\to K\pi$, $B\to KK$, and $B\to\pi\pi$ decays [25]. Subsequently, it is extended to charmless two-body $B\to PP$ decays involving the isosinglet mesons η and η' [30].

In the present work, we extend this method to the $B\to VP$ decays. We will use the wealth of the experimental data to fit the nonperturbative inputs (in our analysis, we also take the $B\to PP$ decays into account). In doing this, we would assume SU(3) symmetry for form factors and charming penguins to reduce the number of independent nonperturbative inputs: there are totally 16 nonperturbative inputs to be determined. Utilizing the meson matrices, we give the master equations for the hard kernels for $B\to M_1M_2$ decays. After analyzing the $B\to VP$ decays at leading power, we take part of chirally enhanced penguin into account. With the chirally enhanced penguins taken into account, we find most of the 16 inputs are not changed sizably except charming penguins. Flavor-singlet mesons η and η' receive additional contributions (gluonic contributions) from a higher Fock state component. In Ref. [30], the gluonic form factors and gluonic charming penguins which are responsible for $B\to PP$ decays are fitted using the related experimental data. Since there are not enough experimental results, the authors find two solutions for these inputs. This situation is changed when considering $B\to VP$ decays since we have more data to give more stringent constraint. Incorporating the $B\to VP$ experimental results for branching fractions and CP asymmetries, we find that our results are consistent with their second solution. We find two solutions for the inputs only responsible for $B\to VP$ decays. One of the solutions for $B\to V$ form factors are smaller than those given in Ref. [23], where the $B\to\rho_L\rho_L$ data (ρ_L denotes a longitudinally polarized meson), $B\to\rho^0\rho^-$ and $B\to\rho^+\rho^-$ branching ratios, and CP asymmetries $S_{\rho^+\rho^-}$ and $C_{\rho^+\rho^-}$, are used. Our second solution for $B\to V$ form factors is more consistent with them. Generally speaking, charming penguins in SCET have a similar role with $(S-P)(S+P)$ annihilation penguin operators in PQCD approach. Both of them are essential to give the correct branching ratios in these two different approaches. But there are indeed some differences in predictions on other parameters such as direct CP asymmetries and mixing-induced CP asymmetries. We also make some comparisons between these two objects.

The paper is organized as follows. $B\to VP$ decay amplitudes at leading power are briefly given in Sec. II. What follows is the factorization analysis in which chirally enhanced penguins are taken into account. In Sec. II, utilizing the rich experimental data on branching fractions and time-dependent CP asymmetry observables, we give two kinds of solutions for the 16 nonperturbative parameters responsible for $B\to PP$ and $B\to VP$ decays at the leading power accuracy. With the inclusion of a chirally enhanced penguin, most parameters remain unchanged except the charming penguin parameters. Predictions on branching fractions and other observables, including direct CP asymmetries, time-dependent CP asymmetries, and ratios of branching fractions, are given subsequently. A comparison between charming penguins in SCET and annihilation diagrams in the PQCD approach is presented in Sec. V. Section VI contains our conclusions. In the appendix, we

give the master equations for the hard kernels in both $b \to d$ and $b \to s$ transitions.

II. $B \to VP$ DECAY AMPLITUDES AT LEADING POWER IN SCET

In this section, we briefly review the factorization analysis at the leading power and collect the corresponding leading order short-distance coefficients. The weak effective Hamiltonian which describes $b \to D$ ($D = d, s$) transitions is [31]

$$\mathcal{H}_{\text{eff}} = \frac{G_F}{\sqrt{2}}\Big\{\sum_{q=u,c} V_{qb}V_{qD}^*[C_1 O_1^q + C_2 O_2^q] - V_{tb}V_{tD}^*\Big[\sum_{i=3}^{10,7\gamma,8g} C_i O_i\Big]\Big\} + \text{H.c.}, \tag{3}$$

where $V_{qb(D)}$ are the CKM matrix elements and in the following we will also use products of the CKM matrix elements $\lambda_q^{(f)}$ ($q = u,\ c,\ t$) defined by $\lambda_q^{(f)} = V_{qb}V_{qf}^*$. Functions O_i ($i = 1, \ldots, 10,\ 7\gamma,\ 8g$) are the local four-quark operators or the moment type operators:

(i) current-current (tree) operators

$$O_1^q = (\bar{q}_\alpha b_\alpha)_{V-A}(\bar{D}_\beta q_\beta)_{V-A},$$
$$O_2^q = (\bar{q}_\alpha b_\beta)_{V-A}(\bar{D}_\beta q_\alpha)_{V-A}, \tag{4}$$

(ii) QCD penguin operators

$$O_3 = (\bar{D}_\alpha b_\alpha)_{V-A}\sum_{q'}(\bar{q}'_\beta q'_\beta)_{V-A},$$
$$O_4 = (\bar{D}_\beta b_\alpha)_{V-A}\sum_{q'}(\bar{q}'_\alpha q'_\beta)_{V-A}, \tag{5}$$

$$O_5 = (\bar{D}_\alpha b_\alpha)_{V-A}\sum_{q'}(\bar{q}'_\beta q'_\beta)_{V+A},$$
$$O_6 = (\bar{D}_\beta b_\alpha)_{V-A}\sum_{q'}(\bar{q}'_\alpha q'_\beta)_{V+A}, \tag{6}$$

(iii) electroweak penguin operators

$$O_7 = \frac{3}{2}(\bar{D}_\alpha b_\alpha)_{V-A}\sum_{q'} e_{q'}(\bar{q}'_\beta q'_\beta)_{V+A},$$
$$O_8 = \frac{3}{2}(\bar{D}_\beta b_\alpha)_{V-A}\sum_{q'} e_{q'}(\bar{q}'_\alpha q'_\beta)_{V+A}, \tag{7}$$

$$O_9 = \frac{3}{2}(\bar{D}_\alpha b_\alpha)_{V-A}\sum_{q'} e_{q'}(\bar{q}'_\beta q'_\beta)_{V-A},$$
$$O_{10} = \frac{3}{2}(\bar{D}_\beta b_\alpha)_{V-A}\sum_{q'} e_{q'}(\bar{q}'_\alpha q'_\beta)_{V-A}, \tag{8}$$

(iv) magnetic moment operators

$$O_{7\gamma} = -\frac{em_b}{4\pi^2}\bar{D}_\alpha \sigma^{\mu\nu} P_R b_\alpha F_{\mu\nu},$$
$$O_{8g} = -\frac{gm_b}{4\pi^2}\bar{D}_\alpha \sigma^{\mu\nu} P_R T^a_{\alpha\beta} b_\beta G^a_{\mu\nu}, \tag{9}$$

where α and β are color indices and q' are the active quarks at the scale m_b, i.e. $q' = (u, d, s, c, b)$. The m_b is the b quark mass and we use $m_b = 4.8$ GeV. The left-handed current is defined as $(\bar{q}'_\alpha q'_\beta)_{V-A} = \bar{q}'_\alpha \gamma_\nu(1 - \gamma_5)q'_\beta$ and the right-handed current $(\bar{q}'_\alpha q'_\beta)_{V+A} = \bar{q}'_\alpha \gamma_\nu(1 + \gamma_5)q'_\beta$. The projection operators are defined as $P_L = (1 - \gamma_5)/2$ and $P_R = (1 + \gamma_5)/2$. The electroweak penguin operators $O_{9,10}$ can be eliminated using $e_q \bar{q}q = \bar{u}u + \bar{c}c - \frac{1}{3}\bar{q}q$. In the following, we will work to leading order in $\alpha_s(m_b)$. In the naive dimensional regularization scheme for $\alpha_s(m_Z) = 0.119$, $\alpha_{\text{em}} = 1/128$, $m_t = 174.3$ GeV, the Wilson coefficients C_i at leading logarithm order for tree and QCD penguin operators are

$$C_{1-6}(m_b) = \{1.110, -0.253, 0.011, -0.026, 0.008, -0.032\}, \tag{10}$$

while the Wilson coefficients for electroweak penguin operators are

$$C_{7-10}(m_b) = \{0.09, 0.24, -10.3, 2.2\} \times 10^{-3}, \tag{11}$$

and for the magnetic operators $C_{7\gamma}(m_b) = -0.315$, $C_{8g}(m_b) = -0.149$. We have used the sign convention for the electromagnetic and strong coupling constant as $D_\mu = \partial_\mu - igT^a A_\mu^a - ieQ_f A_\mu$, so that the Feynman rule for the vertex is $igT^a\gamma_\mu + ieQ_f\gamma_\mu$.

In the present work, we will adopt the notations as in Ref. [32] and use $\lambda = \sqrt{\Lambda_{\text{QCD}}/m_b}$. The emitted quark and antiquark mainly move along the direction n_+ and the recoiling meson is moving on the direction n_-, where $n_\pm$ are two light-cone vectors: $n_\pm^2 = 0$ and $n_+ \cdot n_- = 2$. The matching from QCD onto SCET are always performed in two stages. We will first integrate out the fluctuations with off-shellness $\mathcal{O}(m_b^2)$ to give the intermediate effective theory. At the final stage, we integrate out the hard-collinear modes with off-shellness $\mathcal{O}(m_b\Lambda_{\text{QCD}})$ to derive SCET$_{II}$.

A. Matching onto SCET$_I$

To study the decay amplitudes of $B \to M_1 M_2$ decays in SCET, we first consider the possible operators using the building blocks. The power counting rule for these blocks has been given in Ref. [32]. Integrating out the hard scales with typical off-shellness m_b^2, the electroweak operators can match onto two kinds of operators in SCET where the situation is similar with that in B to light form factors: the first kind of operators involve four quark fields while the

second one involves an additional transverse gluon field. For flavor-singlet mesons, one needs to consider the operators which are composed by two gluon fields. Then the leading power operators responsible for $b \to s$ transitions are chosen by

$$\begin{aligned}
Q_{1s}^{(0)}(t) &= \left[(\bar{s}W_{c2})(tn_-)\frac{\not{n}_-}{2}(1-\gamma_5)(W_{c2}^\dagger u)\right][(\bar{u}W_{c1})\not{n}_+(1-\gamma_5)h_v], \\
Q_{2s,3s}^{(0)}(t) &= \left[(\bar{u}W_{c2})(tn_-)\frac{\not{n}_-}{2}(1\mp\gamma_5)(W_{c2}^\dagger u)\right][(\bar{s}W_{c1})\not{n}_+(1-\gamma_5)h_v], \\
Q_{4s}^{(0)}(t) &= \left[(\bar{s}W_{c2})(tn_-)\frac{\not{n}_-}{2}(1-\gamma_5)(W_{c2}^\dagger q)\right][(\bar{q}W_{c1})\not{n}_+(1-\gamma_5)h_v], \\
Q_{5s,6s}^{(0)}(t) &= \left[(\bar{q}W_{c2})(tn_-)\frac{\not{n}_-}{2}(1\mp\gamma_5)(W_{c2}^\dagger q)\right][(\bar{s}W_{c1})\not{n}_-n_+(1-\gamma_5)h_v], \\
Q_{gs}^{(0)}(t) &= m_b i\epsilon_{\perp\mu\nu}\,\mathrm{Tr}[[W_{c2}^\dagger iD_{\perp c2}^\mu W_{c2}](tn_-)[W_{c2}^\dagger iD_{\perp c2}^\nu W_{c2}]][(\bar{s}W_{c1})\not{n}_+(1-\gamma_5)h_v],
\end{aligned} \tag{12}$$

with the trace over the color indices. The operators suppressed by λ are given by

$$\begin{aligned}
Q_{1s}^{(1)}(t,s) &= -\frac{1}{m_b}\left[(\bar{s}W_{c2})(tn_-)\frac{\not{n}_-}{n_-v}(1-\gamma_5)(W_{c2}^\dagger u)\right][(\bar{u}W_{c1})(W_{c1}^\dagger i\not{D}_{\perp c1}W_{c1})(sn_+)(1-\gamma_5)h_v], \\
Q_{2s,3s}^{(1)}(t,s) &= -\frac{1}{m_b}\left[(\bar{u}W_{c2})(tn_-)\frac{\not{n}_-}{n_-v}(1\mp\gamma_5)(W_{c2}^\dagger u)\right][(\bar{s}W_{c1})(W_{c1}^\dagger i\not{D}_{\perp c1}W_{c1})(sn_+)(1-\gamma_5)h_v\Big], \\
Q_{4s}^{(1)}(t,s) &= -\frac{1}{m_b}\left[(\bar{s}W_{c2})(tn_-)\frac{\not{n}_-}{n_-v}(1-\gamma_5)(W_{c2}^\dagger q)\right][(\bar{q}W_{c1})(W_{c1}^\dagger i\not{D}_{\perp c1}W_{c1})(sn_+)(1-\gamma_5)h_v], \\
Q_{5s,6s}^{(1)}(t,s) &= -\frac{1}{m_b}\left[(\bar{q}W_{c2})(tn_-)\frac{\not{n}_-}{n_-v}(1\mp\gamma_5)(W_{c2}^\dagger q)\right][(\bar{s}W_{c1})(W_{c1}^\dagger i\not{D}_{\perp c1}W_{c1})(sn_+)(1-\gamma_5)h_v], \\
Q_{7s}^{(1)}(t,s) &= -\frac{1}{m_b}[(\bar{s}W_{c2})(tn_-)\not{n}_-\gamma_\mu^\perp(1+\gamma_5)(W_{c2}^\dagger u)][(\bar{u}W_{c1})(W_{c1}^\dagger iD_{\perp c1}^\mu W_{c1})(sn_+)(1-\gamma_5)(sn_+)h_v], \\
Q_{8s}^{(1)}(t,s) &= -\frac{1}{m_b}[(\bar{s}W_{c2})(tn_-)\not{n}_-\gamma_\mu^\perp(1+\gamma_5)(W_{c2}^\dagger q)][(\bar{q}W_{c1})(W_{c1}^\dagger iD_{\perp c1}^\mu W_{c1})(sn_+)(1-\gamma_5)h_v], \\
Q_{gs}^{(1)}(t,s) &= -2m_b i\epsilon_{\perp\mu\nu}\mathrm{Tr}[[W_{c2}^\dagger iD_{\perp c2}^\mu W_{c2}](tn_-)[W_{c2}^\dagger iD_{\perp c2}^\nu W_{c2}]][(\bar{s}W_{c1})(W_{c1}^\dagger i\not{D}_{\perp c1}W_{c1})(sn_+)(1-\gamma_5)h_v],
\end{aligned} \tag{13}$$

where the fields without position argument are at $x = 0$. The field products within the square brackets are color-singlet and we will neglect the color-octet operators since they give vanishing matrix elements at leading order. The operators responsible for $b \to d$ transitions could be directly obtained by replacing s quark fields by the corresponding d quark fields. Although the operators given in Eq. (13) are suppressed by λ compared with those in Eq. (12), all of the operators in Eqs. (12) and (13) contribute to $\langle M_1 M_2|O|B\rangle$ at the same power when matching onto $\mathrm{SCET_{II}}$. Hence the effective Hamiltonians are matched onto $\mathrm{SCET_I}$ by the following equation:

$$\mathcal{H}_{\mathrm{eff}} = \frac{G_F}{\sqrt{2}}\left\{\int d\hat{t}\hat{c}_i(\hat{t})O_i^{(0)}(t) + \int d\hat{t}d\hat{s}\hat{b}_i(\hat{t},\hat{s})O_i^{(1)}(t,s)\right\}, \tag{14}$$

with $\hat{s} = n_+ \cdot p's = m_B s$, $\hat{t} = n_- \cdot qt = m_B t$ (p' and q are the momentum of the recoiling and emitted meson, respectively). We usually evaluate the Wilson coefficients $c_i(u)$ and $b_i(u,z)$ in momentum space which is related to the ones in coordinated space by

$$\begin{aligned}
c_i(u) &= \int d\hat{t}e^{-ium_B\hat{t}}\hat{c}_i(\hat{t}), \\
b_i(u,z) &= \int d\hat{t}e^{-im_B(u\hat{t}+z\hat{s})}\hat{b}_i(\hat{t},\hat{s}).
\end{aligned} \tag{15}$$

The tree-level matching coefficients for the four-body operators in Eq. (12) are given by

$$\begin{aligned}
c_{1,2}^{(f)} &= \lambda_u^{(f)}\left[C_{1,2} + \frac{1}{N_c}C_{2,1}\right] - \lambda_t^{(f)}\frac{3}{2}\left[\frac{1}{N_c}C_{9,10} + C_{10,9}\right], \\
c_3^{(f)} &= -\frac{3}{2}\lambda_t^{(f)}\left[C_7 + \frac{1}{N_c}C_8\right], \\
c_{4,5}^{(f)} &= -\lambda_t^{(f)}\left[\frac{1}{N_c}C_{3,4} + C_{4,3} - \frac{1}{2N_c}C_{9,10} - \frac{1}{2}C_{10,9}\right], \\
c_6^{(f)} &= -\lambda_t^{(f)}\left[C_5 + \frac{1}{N_c}C_6 - \frac{1}{2}C_7 - \frac{1}{2N_c}C_8\right], \\
c_g^{(f)} &= 0.
\end{aligned} \tag{16}$$

The tree level matching of five-body operators leads to

$$
\begin{aligned}
b_{1,2}^{(f)} &= \lambda_u^{(f)}\Big[C_{1,2} + \frac{1}{N_c}\Big(1 - \frac{m_b}{\omega_3}\Big)C_{2,1}\Big] \\
&\quad - \lambda_t^{(f)}\frac{3}{2}\Big[C_{10,9} + \frac{1}{N_c}\Big(1 - \frac{m_b}{\omega_3}\Big)C_{9,10}\Big], \\
b_3^{(f)} &= -\lambda_t^{(f)}\frac{3}{2}\Big[C_7 + \Big(1 - \frac{m_b}{\omega_2}\Big)\frac{1}{N_c}C_8\Big], \\
b_{4,5}^{(f)} &= -\lambda_t^{(f)}\Big[C_{4,3} + \frac{1}{N_c}\Big(1 - \frac{m_b}{\omega_3}\Big)C_{3,4}\Big] \\
&\quad + \lambda_t^{(f)}\frac{1}{2}\Big[C_{10,9} + \frac{1}{N_c}\Big(1 - \frac{m_b}{\omega_3}\Big)C_{9,10}\Big], \\
b_6^{(f)} &= -\lambda_t^{(f)}\Big[C_5 + \frac{1}{N_c}\Big(1 - \frac{m_b}{\omega_2}\Big)C_6\Big] \\
&\quad + \lambda_t^{(f)}\frac{1}{2}\Big[C_7 + \frac{1}{N_c}\Big(1 - \frac{m_b}{\omega_2}\Big)C_8\Big], \\
b_7^{(f)} &= -\lambda_t^{(f)}\frac{3}{2}C_7\frac{1}{N_c}\Big(\frac{m_b}{\omega_2} - \frac{m_b}{\omega_3}\Big), \\
b_8^{(f)} &= -\lambda_t^{(f)}\Big(C_5 - \frac{1}{2}C_7\Big)\frac{1}{N_c}\Big(\frac{m_b}{\omega_2} - \frac{m_b}{\omega_3}\Big), \\
b_g^{(f)} &= \lambda_t^{(f)}C_{8g}\frac{\alpha_s(m_b)}{16C_F}\Big(\frac{1}{\bar{u}} - \frac{1}{u}\Big) \\
&\quad \times\Big[\frac{2+z}{1-z} + 2\Big(1 - \frac{1}{N_c^2}\Big)\frac{u\bar{u}}{(1-zu)(1-z\bar{u})}\Big],
\end{aligned}
\tag{17}
$$

where $\omega_2 = um_B$ and $\omega_3 = -\bar{u}m_B$ with u is the momentum fraction of the positive quark in the emitted meson. m_B is the B-meson mass. $C_F = (N_c^2 - 1)/2N_c$ and $N_c = 3$. The one-loop corrections are given in Refs. [8,9,19,21–23]. The coefficients c_g^f and b_g^f are zero at $\mathcal{O}(\alpha_s^0)$, thus they are not relevant for the present study in which we concentrate on the leading order analysis.

In $\mathrm{SCET_I}$, the matrix elements of $O_i^{(0,1)}$ can be decomposed into some simple and universal ones defined as follows:

$$
\begin{aligned}
&\langle M_1|(\bar{\chi}W_{c2})(tn_-)\frac{\not{n}_-}{2}(1-\gamma_5)(W_{c2}^\dagger\chi)|0\rangle \\
&\quad = \frac{if_{M_1}m_B}{2}\int_0^1 du e^{iu\hat{t}}\phi_{M_1}(u), \\
&\langle M_2|T[(\bar{\chi}W_{c1})\not{n}_+(1-\gamma_5)h_v]|B\rangle = m_B\zeta, \\
&\langle M_2|T[(\bar{u}W_{c1})(W_{c1}^\dagger i\not{D}_{\perp c1}W_{c1})(sn_+)(1-\gamma_5)h_v]|B\rangle \\
&\quad = -m_B^2\int dz e^{im_Bz\cdot s}\zeta_J(z),
\end{aligned}
\tag{18}
$$

where M_2 is an arbitrary pseudoscalar meson or vector meson except η and η'.

B. Matching to $\mathrm{SCET_{II}}$

The matching of $\mathrm{SCET_I}$ onto $\mathrm{SCET_{II}}$ is performed by integrating out the degrees of freedom with $p^2 \sim \Lambda m_b$. To do so, it is useful to perform a redefintion of collinear fields: $q \to Y_s q$, where Y_s is a soft Wilson line. The SCET Lagrangian contains no leading order interactions between the collinear-2 and collinear-1 fields after decoupling soft gluons from a collinear-2 sector by a field redefinition. Although soft Wilson lines still appear in the effective electroweak operators, the Wilson line only appears in the combination of $Y_s h_v$. Thus the two kinds of collinear sectors decouple and the decay amplitudes factorize.

In $\mathrm{SCET_{II}}$, the end-point singularity prevents the factorization of ζ while the form factor $\zeta_J^{BM}(z)$ can be further factorized into a convolution of light-cone-distribution amplitudes (LCDAs) and jet functions:

$$
\zeta_J^{BM}(z) = \frac{f_B f_M}{m_B}\int dk_+ dx \phi_B^+(k_+)J(z,x,k_+)\phi_M(x). \tag{19}
$$

At the lowest order, $J(z,x,k_+) = \delta(z-x)\alpha_s\pi C_F/(N_c\bar{x}k_+)$.

C. Decay amplitudes involving flavor-singlet mesons η and η'

For isosinglet mesons η and η', we adopt the Feldmann-Kroll-Stech mixing scheme [33–35]. In this scheme, an arbitrary isosinglet biquark operator O can be written as a linear combination of $O_q \sim (u\bar{u} + d\bar{d})/\sqrt{2}$ and $O_s \sim s\bar{s}$ operators with the well-defined flavor structure. Matrix elements of $O = c_q O_q + c_s O_s$ between η, η' states and the vacuum state can be parameterized by

$$
\langle 0|O|\eta\rangle = c_q\cos\phi_q\langle O_q\rangle - c_s\sin\phi_s\langle O_s\rangle, \tag{20}
$$

$$
\langle 0|O|\eta'\rangle = c_q\sin\phi_q\langle O_q\rangle + c_s\cos\phi_s\langle O_s\rangle, \tag{21}
$$

where the four matrix elements $\langle 0|O_{q,s}|\eta^{(\prime)}\rangle$ are expressed by the two angles $\phi_{q,s}$ and two reduced matrix elements $\langle O_{q,s}\rangle$. Phenomenologically, one can neglect the OZI (Okubo-Zweig-Iizuka) suppressed matrix elements and obtain $\phi_q = \phi_s = \theta$. Thus, the mass eigenstates η, η' are related to the flavor basis through

$$
\eta = \eta_q\cos\theta - \eta_s\sin\theta, \qquad \eta' = \eta_q\sin\theta + \eta_s\cos\theta. \tag{22}
$$

For these isosinglet mesons η_q and η_s, we need in addition more theoretical inputs which arise from the higher Fock state component:

$$
\begin{aligned}
&i\epsilon_{\perp\mu\nu}\langle\eta_q(p)|\mathrm{Tr}[[W_{c2}^\dagger iD_{\perp c2}^\mu W_{c2}](tn_-)[W_{c2}^\dagger iD_{\perp c2}^\nu W_{c2}]]|0\rangle = \int_0^1 du e^{iu\hat{t}}\frac{i}{4}\sqrt{C_F}\sqrt{\frac{2}{3}}f_{\eta_q}\bar{\Phi}_P^g(u),\\
&i\epsilon_{\perp\mu\nu}\langle\eta_s(p)|\mathrm{Tr}[[W_{c2}^\dagger iD_{\perp c2}^\mu W_{c2}](tn_-)[W_{c2}^\dagger iD_{\perp c2}^\nu W_{c2}]]|0\rangle = \int_0^1 du e^{iu\hat{t}}\frac{i}{4}\sqrt{C_F}\sqrt{\frac{1}{3}}f_{\eta_s}\bar{\Phi}_P^g(u),\\
&(\langle\eta_q|T[(\bar{\chi}W_{c1})\not{n}_+(1-\gamma_5)h_v]|B\rangle)_g = \sqrt{2}m_B\zeta_g, \qquad (\langle\eta_s|T[(\bar{\chi}W_{c1})\not{n}_+(1-\gamma_5)h_v]|B\rangle)_g = m_B\zeta_g,\\
&(\langle\eta_q|T[(\bar{\chi}W_{c1})(W_{c1}^\dagger i\not{D}_{\perp c1}W_{c1})(sn_+)(1-\gamma_5)h_v]|B\rangle)_g = -\sqrt{2}m_B^2\int dz e^{im_Bz\cdot s}\zeta_{Jg}(z),\\
&(\langle\eta_s|T[(\bar{\chi}W_{c1})(W_{c1}^\dagger i\not{D}_{\perp c1}W_{c1})(sn_+)(1-\gamma_5)h_v]|B\rangle)_g = -m_B^2\int dz e^{im_Bz\cdot s}\zeta_{Jg}(z),
\end{aligned}
\tag{23}
$$

where only the gluonic contributions to $B\to\eta_q$, η_s form factors are shown. Note that our convention is different from the one used in Ref. [30], where the form factors ζ_g and ζ_{Jg} are incorporated in the definition of $\zeta_{(J)}^{BM_2}$. Here we have separated them out and the two functions $\zeta_{(J)}^{BM_2}$ do not contain contributions from the gluonic term. This convention is more convenient when extracting the hard kernels using master equations given in the appendix.

In $\mathrm{SCET_{II}}$, ζ_g cannot be factorized either for the presence of end-point singularity but $\zeta_{Jg}^{BM}(z)$ is given in terms of the jet functions by

$$
\zeta_{Jg}^{BM}(z) = \frac{f_Bf_M}{m_B}\frac{1}{4}\sqrt{\frac{C_F}{3}}\int dk_+dx\phi_B^+(k_+)J_g(z,x,k_+)\bar{\Phi}_M^g(x),
\tag{24}
$$

At the lowest order, $J_g(z,x,k_+)=\delta(z-x)\alpha_s2\pi/(N_ck_+)$.

D. A summary of the factorization formulas

In summary, the $b\to s(d)$ decay amplitudes at leading power in SCET can be expressed by

$$
\begin{aligned}
A(B\to M_1M_2) = \frac{G_F}{\sqrt{2}}m_B^2\Big\{&f_{M_1}\int du\phi_{M_1}(u)T_1(u)\zeta^{BM_2} + f_{M_1}\int du\phi_{M_1}(u)\int dzT_{1J}(u,z)\zeta_J^{BM_2}(z)\\
&+ f_{M_1}\int du\phi_{M_1}(u)T_{1g}(u)\zeta_g^{BM_2} + f_{M_1}\int du\phi_{M_1}(u)\int dzT_{1Jg}(u,z)\zeta_{Jg}^{BM_2}(z)\\
&+ f_{M_1}^1\int du\bar{\Phi}_{M_1}^g(u)T_1^g(u)\zeta^{BM_2} + f_{M_1}^1\int du\bar{\Phi}_{M_1}^g(u)\int dzT_{1J}^g(u,z)\zeta_J^{BM_2}(z) + f_{M_1}^1\int du\bar{\Phi}_{M_1}^g(u)T_{1g}^g(u)\zeta_g^{BM_2}\\
&+ f_{M_1}^1\int du\bar{\Phi}_{M_1}^g(u)\int dzT_{1Jg}^g(u,z)\zeta_{Jg}^{BM_2}(z) + \lambda_c^{(f)}A_{cc}^{M_1M_2} + (1\leftrightarrow 2)\Big\},
\end{aligned}
\tag{25}
$$

where $A_{cc}^{M_1M_2}$ denotes the nonperturbative charming penguins. T_i are hard kernels which can be calculated using perturbation theory. In the appendix, based on the flavor structure of the four-body operators and five-body operators, we give the master equations for hard kernels T_i which utilize the coefficients given in Eqs. (16) and (17). For distinct decay channels, one can easily evaluate the equation to obtain the corresponding hard kernels.

In SCET, the factorization formula for $B\to M_1M_2$ is easily proved to hold to all orders in α_s: the amplitudes given in Eq. (25) have the form of a convolution of the universal light-cone distribution amplitudes and the perturbative hard kernels. Utilizing the perturbative expansion in $\alpha_s(\sqrt{m_b\Lambda})$ for the jet functions and in $\alpha_s(m_b)$ for the Wilson coefficients, one can predict the branching ratios, CP asymmetries, and other observables for $B\to M_1M_2$ decays. One can also use another parallel method: the nonperturbative parameters can be fitted by experimental measurements on the $B\to M_1M_2$ decays. This approach is especially useful at leading order in α_s, since then the hard kernels $T_1(u)$ are constants, while $T_{1J}(u,z)$ are functions of u only. Furthermore, at this order terms with hard kernels $T_{1J}^g(u,z)$, $T_1^g(u)$, $T_{1Jg}^g(u,z)$, $T_{1g}^g(u)$ do not contribute at all. Thus the decay amplitudes of $B\to M_1M_2$ decays at leading order in $\alpha_s(m_b)$ are written by

$$
\begin{aligned}
A(B\to M_1M_2) = \frac{G_F}{\sqrt{2}}m_B^2\Big\{&f_{M_1}\Big[\zeta_J^{BM_2}\int du\phi_{M_1}(u)T_{1J}(u)\\
&+ \zeta_{Jg}^{BM_2}\int du\phi_{M_1}(u)T_{1Jg}(u)\Big]\\
&+ f_{M_1}(T_1\zeta^{BM_2} + T_{1g}\zeta_g^{BM_2}) + \lambda_c^{(f)}A_{cc}^{M_1M_2}\\
&+ (1\leftrightarrow 2)\Big\},
\end{aligned}
\tag{26}
$$

where the four functions ζ^{BM_1}, ζ_g and

$$
\zeta_J^{BM_2} = \int dz\zeta_J^{BM_2}(z), \qquad \zeta_{Jg}^{BM_2} = \int dz\zeta_{Jg}^{BM_2}(z),
\tag{27}
$$

are treated as nonperturbative parameters to be fitted from experiment measurements.

In order to reduce the independent inputs, one can utilize the SU(3) symmetry for B to light form factors and charming penguins. In the exact SU(3) limit, only two form factors are needed for $B \to PP$ decays without isosinglet mesons:

$$\zeta^{BP}_{(J)} \equiv \zeta^{B\pi}_{(J)} = \zeta^{BK}_{(J)} = \zeta^{B_sK}_{(J)}. \tag{28}$$

Besides these two form factors, there are two additional new nonperturbative functions $\zeta_{(J)g}$ in decays involving isosinglet mesons η_q and η_s. They are contributions from the intrinsic gluons. The $B \to V$ form factors are rather simple, since there is no gluonic contribution at all. The flavor SU(3) symmetry implies the relation for $B \to V$ form factors:

$$\zeta^{BV}_{(J)} \equiv \zeta^{B\rho}_{(J)} = \zeta^{BK^*}_{(J)} = \zeta^{B\omega}_{(J)} = \zeta^{B_sK^*}_{(J)} = \zeta^{B_s\phi}_{(J)}. \tag{29}$$

If the SU(3) symmetry is assumed for charming penguins, there are totally five complex charming penguins which depend on the spin and isospin properties of the emitted mesons and recoiling mesons: A^{PP}_{cc}, A^{PV}_{cc}, A^{VP}_{cc}, A^{PP}_{ccg}, A^{VP}_{ccg}. $A^{M_1M_2}_{cc}$ denotes the charming penguins in which the M_1 meson is emitted and the M_2 meson is recoiled. The two charming penguins A^{PP}_{ccg}, A^{VP}_{ccg} only contribute to decays in which a isosinglet meson is recoiled.

With the assumption of flavor SU(3) symmetry for B to light form factors and charming penguin terms, the nonperturbative, totally 16 real inputs responsible for $B \to PP$ and $B \to VP$ decays are summarized in the following:

$$\zeta^{BP}, \zeta^{BP}_J, \zeta_g, \zeta_{Jg}, \zeta^{BV}, \zeta^{BV}_J, A^{PP}_{cc}, A^{PV}_{cc}, A^{VP}_{cc}, A^{PP}_{ccg}, A^{VP}_{ccg}. \tag{30}$$

III. CHIRALLY ENHANCED PENGUINS

Power corrections are expected to be suppressed by at least the factor $\Lambda_{\rm QCD}/m_b$, but chirally enhanced penguins are large enough to compete with the leading power QCD penguins as the suppression factor becomes $2\mu_P/m_b$, where $\mu_P \sim 2$ GeV is the chiral scale parameter. Thus in both of QCDF [8–10] and PQCD [11–13] approaches, it has been incorporated in the phenomenological analysis. In the framework of SCET, the complete operator basis and the corresponding factorization formulas for the chirally enhanced penguin are recently derived in Refs. [23,24] and the amplitudes do not suffer from additional end-point singularities. The factorization formula will introduce a new form factor ζ_χ and a new light-cone distribution amplitude ϕ^{pp}.

As discussed in Ref. [23], there are three different kinds of chirally enhanced penguin operators in $\mathrm{SCET_I}$: $Q^{1\chi}_A$, $Q^{(1\chi)}_B$, and $Q^{(2\chi)}_B$. The basis for the $Q^{(1\chi)}_A$-type operators is given by

$$Q^{(1\chi)}_{1(qfq)} = \frac{1}{m_b}[(\bar q W_{c1})(1-\gamma_5)h_v] \times \left[(\bar s W_{c2})(tn_-)\frac{\not n_-}{n_-v} i\not\partial_\perp (1+\gamma_5)(W^\dagger_{c2}q)\right],$$
$$Q^{(1\chi)}_{2(qfq)} = Q^{(1\chi)}_{1(qfq)}\frac{3}{2}e_q. \tag{31}$$

These two operators $Q^{(1\chi)}_{1,2}$ will contribute to $B \to PP$, VP, V_LV_L decays (here V_L denotes a longitudinally polarized vector meson). There are in addition several operators omitted here, as they can only contribute to $B \to V_TV_T$ decays (V_T denotes a transversely polarized vector meson). The second kind of operators which are responsible for $B \to PP$, VP, V_LV_L decays are given by

$$Q^{(2\chi)}_{1(qfq)} = \frac{-1}{m_b}\Big[(\bar q W_{c1})\frac{1}{n_+\cdot i\partial} i\partial_\perp \cdot (W^\dagger_{c1} iD_{\perp c1} W_{c1})(sn_+)(1+\gamma_5)h_v\Big] \times [(\bar s W_{c2})(tn_-)\not n_-(1-\gamma_5)(W^\dagger_{c2}q)], \tag{32}$$

$$Q^{(2\chi)}_{2(fuu)} = \frac{-1}{m_b}\Big[(\bar s W_{c1})\frac{1}{n_+\cdot i\partial} i\partial_\perp \cdot (W^\dagger_{c1} iD_{\perp c1} W_{c1})(sn_+)(1+\gamma_5)h_v\Big] \times [(\bar u W_{c2})(tn_-)\not n_-(1+\gamma_5)(W^\dagger_{c2}u)], \tag{33}$$

$$Q^{(2\chi)}_{3(qfq)} = \frac{-1}{m_b^2}[(\bar q W_{c1})(W^\dagger_{c1} i\not D_{\perp c1} W_{c1})(sn_+)(1-\gamma_5)h_v] \times \left[(\bar s W_{c2})(tn_-)\frac{\not n_-}{n_-v} i\not\partial_\perp (1+\gamma_5)(W^\dagger_{c2}q)\right], \tag{34}$$

$$Q^{(2\chi)}_{4(qfq)} = \tfrac{3}{2}e_q Q^{(2\chi)}_{3(qfq)}, \tag{35}$$

plus operators with the same Dirac structure but different flavors, $Q^{(2\chi)}_{1(ufu)}$ and $Q^{(2\chi)}_{1(fuu)}$. If n_--iso-singlet operators are included, we have two additional operators $Q^{(2\chi)}_{1(fqq)}$ and $Q^{(2\chi)}_{2(fqq)}$. Operators $Q^{(2\chi)}_{1-4}$ contribute to $B \to PP$, VP, V_LV_L decays, while operators which only contribute to $B \to V_TV_T$ decays are also given in Ref. [23] but omitted here, since we mainly concentrate on $B \to PP$ and $B \to VP$ decays.

Matching from QCD to $\mathrm{SCET_I}$, one obtains the effective Hamiltonian expressed by the (1χ) and (2χ)-type operators contributing to $B \to PP$, VP, V_LV_L decays:

$$\mathcal{H}^{\chi}_{\rm eff} = \frac{G_F}{\sqrt{2}}\Big[\int d\hat t \hat c^{\chi}_{i(F)}(\hat t) Q^{(1\chi)}_{i(F)}(t) + \int d\hat t d\hat s \hat b^{\chi}_{i(F)}(\hat t,\hat s) Q^{(2\chi)}_{i(F)}(t,s)\Big], \tag{36}$$

where the indices run over the operator number i and possibilities for the flavors F for the $Q_{i(F)}$. $\hat{c}^{\chi}_{i(F)}$ and $\hat{b}^{\chi}_{i(F)}$ are the short-distance Wilson coefficients in coordinate space. At tree level, the corresponding coefficients in momentum space are

$$\begin{aligned}
c^{\chi}_{1(qfq)} &= \lambda_t^{(f)}\Big(C_6+\frac{C_5}{N_c}\Big)\frac{1}{u\bar{u}},\\
c^{\chi}_{2(qfq)} &= \lambda_t^{(f)}\Big(C_8+\frac{C_7}{N_c}\Big)\frac{1}{u\bar{u}},\\
b^{\chi}_{1(qfq)} &= \lambda_t^{(f)}\Big[\frac{1+uz}{uz}\Big(\frac{C_3}{N_c}-\frac{C_9}{2N_c}\Big)+C_4-\frac{C_{10}}{2}\Big],\\
b^{\chi}_{2(fuu)} &= 3\lambda_t^{(f)}\Big[C_7+\frac{C_8}{N_c}-\frac{C_8}{\bar{u}zN_c}\Big],\\
b^{\chi}_{1(ufu)} &= \frac{2(1+uz)}{uz}\Big(-\frac{C_2}{N_c}\lambda_u^{(f)}+\frac{3C_9}{2N_c}\lambda_t^{(f)}\Big)\\
&\quad-(2C_1\lambda_u^{(f)}-3C_{10}\lambda_t^{(f)}),\\
b^{\chi}_{1(fuu)} &= \frac{2(1+uz)}{uz}\Big(-\frac{C_1}{N_c}\lambda_u^{(f)}+\frac{3C_{10}}{2N_c}\lambda_t^{(f)}\Big)\\
&\quad-(2C_2\lambda_u^{(f)}-3C_9\lambda_t^{(f)}),\\
b^{\chi}_{3(qfq)} &= \lambda_t^{(f)}\Big(C_6+\frac{C_5}{N_c}\Big)\frac{1}{u\bar{u}},\\
b^{\chi}_{4(qfq)} &= \lambda_t^{(f)}\Big(C_8+\frac{C_7}{N_c}\Big)\frac{1}{u\bar{u}}.
\end{aligned}\tag{37}$$

Matrix elements for these operators can be parametrized into the following universal distributions:

$$\begin{aligned}
&\langle M|\Big[(\bar{q}W_{c1})\frac{1}{\bar{n}\cdot i\partial}i\partial_\perp\cdot(W^\dagger_{c1}iD_{\perp c1}W_{c1})(sn_+)(1+\gamma_5)h_v\Big]|\bar{B}\rangle\\
&=-\frac{\mu_M m_B}{6}\int dz e^{im_B z\cdot s}\zeta^{BM}_{\chi}(z),\\
&\langle M(p)|\Big[(\bar{s}W_{c2})(tn_-)\frac{\not{n}_-}{n_-\upsilon}i\not{\partial}_\perp(1+\gamma_5)(W^\dagger_{c2}q)\Big]|0\rangle\\
&=-\frac{if_M\mu_M}{3}\int_0^1 du e^{iu\hat{t}}\phi_M^{pp}(u),
\end{aligned}\tag{38}$$

where μ_M is the chiral scale parameter which is set to zero for vector mesons. Using equation of motion, the pseudoscalar's light-cone distribution amplitude $\phi_P^{pp}(u)$ can be related to ones defined in QCD [24,36]:

$$\phi_P^{pp}(u)=3u\Big[\phi_p+\frac{\phi'_\sigma}{6}+\frac{2f_{3P}}{f_P\mu_P}\int\frac{d\upsilon}{\upsilon}\phi_{3P}(u-\upsilon,u)\Big].\tag{39}$$

In the Wandzura-Wilczek approximation, ϕ_{3P} vanishes and one gets $\phi_P^{pp}(u)=6u(1-u)$ for the asymptotic form. With the above matrix elements, generic decay amplitudes from the chiral enhanced penguin could be written as

$$\begin{aligned}
A^{\chi}(B\to M_1M_2)=\frac{G_F}{\sqrt{2}}m_B^2\Big\{&-\frac{\mu_{M_1}f_{M_1}}{3m_B}\int du\phi_{pp}^{M_1}(u)T_1^{\chi}(u)\zeta^{BM_2}-\frac{\mu_{M_1}f_{M_1}}{3m_B}\int dudz\phi_{pp}^{M_1}(u)T_{1J}^{\chi}(u,z)\zeta_J^{BM_2}(z)\\
&-\frac{\mu_{M_1}f_{M_1}}{3m_B}\int du\phi_{pp}^{M_1}(u)T_{1g}^{\chi}(u)\zeta_g^{BM_2}-\frac{\mu_{M_1}f_{M_1}}{3m_B}\int dudz\phi_{pp}^{M_1}(u)T_{1Jg}^{\chi}(u,z)\zeta_{Jg}^{BM_2}(z)\\
&-\frac{\mu_{M_2}f_{M_1}}{6m_B}\int dudz\phi^{M_1}(u)T_{\chi}(u,z)\zeta_{\chi}^{BM_2}(z)+(1\leftrightarrow 2)\Big\},
\end{aligned}\tag{40}$$

where $\zeta_\chi(z)$ can be expressed as convolutions of LCDAs and jet functions:

$$\begin{aligned}
\zeta_{\chi}^{BM}(z)=&\frac{f_Bf_M}{m_b}\int_0^1 dx\int_0^\infty dk^+\frac{J_\perp(z,k^+,x)}{1-z}\\
&\times\phi_B^+(k^+)\phi_{pp}^M(x).
\end{aligned}\tag{41}$$

Here $J_\perp(z,x,k_+)=\delta(x-z)\pi\alpha_sC_F/(N_c\bar{x}k_+)$ at lowest order.

As emphasized in Sec. II, the leading power SCET phenomenological analysis is very useful especially at tree level. It does simplify the analysis. Even taking into account the first four terms in Eq. (40), the scheme for phenomenological studies will remain. But considering the chirally enhanced penguins, the factorization formulas involve a new form factor ζ_χ which cannot be simplified into a normalization constant even at tree level. As shown in Ref. [23], the fifth term proportional to ζ_χ is small which does not give sizable contributions. Thus in our analysis, we neglect it and only consider the first four terms:

$$\begin{aligned}
A^{\chi}(B\to M_1M_2)=&\pm\frac{G_F}{\sqrt{2}}m_B^2\Big(-\frac{2\mu_{M_1}f_{M_1}}{m_B}\Big)\\
&\times\{T_1^{\chi}\zeta^{BM_2}+T_{1J}^{\chi}\zeta_J^{BM_2}+T_{1g}^{\chi}\zeta_g^{BM_2}\\
&+T_{1Jg}^{\chi}\zeta_{Jg}^{BM_2}+(1\leftrightarrow 2)\}.
\end{aligned}\tag{42}$$

For $B\to PP$ decays, the chirally enhanced penguin takes a plus sign; while in $B\to VP$ decays, when emitting a pseudoscalar meson, the amplitude take a minus sign; when a vector meson is emitted, there is no contribution from a chirally enhanced penguin since $\mu_V=0$.

IV. NUMERICAL ANALYSIS OF $B \to VP$ DECAYS

A. Input parameters

In the factorization formulas, we will use the following values for decay constants of the light pseudoscalars and vector mesons (in units of GeV):

$$f_\pi = 0.131, \quad f_K = 0.160, \quad f_{\eta_q} = 1.07 f_\pi = 0.140,$$
$$f_{\eta_s} = 1.34 f_\pi = 0.176, \quad f_\rho = 0.209, \quad f_{K^*} = 0.217,$$
$$f_\omega = 0.195, \quad f_\phi = 0.231. \tag{43}$$

The mixing angle between η_q and η_s is chosen as $\theta = 39.3°$ [33–35]. For the CKM matrix elements and CKM angles, we use the updated global fit results from the CKMfitter group [37]:

$$V_{ud} = 0.97400, \quad V_{us} = 0.22653,$$
$$|V_{ub}| = (3.57^{+0.17}_{-0.17}) \times 10^{-3}, \quad V_{cd} = -0.22638,$$
$$V_{cs} = 0.97316, \quad V_{cb} = (40.5^{+3.2}_{-2.9}) \times 10^{-3},$$
$$|V_{td}| = (8.68^{+0.25}_{-0.33}) \times 10^{-3}, \quad |V_{ts}| = (40.7^{+0.9}_{-0.8}) \times 10^{-3},$$
$$V_{tb} = 0.999135, \quad \beta = (21.7^{+0.017}_{-0.017})°,$$
$$\gamma = (67.6^{+2.8}_{-4.5})°, \quad \epsilon = (1.054^{+0.049}_{-0.051})°. \tag{44}$$

For the inverse moments of light-cone distribution amplitudes for pseudoscalar mesons, we use the same value as in Ref. [30]:

$$\langle x^{-1} \rangle_\pi = \langle x^{-1} \rangle_{\eta_q} = \langle x^{-1} \rangle_{\eta_s} = 3.3,$$
$$\langle x^{-1} \rangle_K = 3.24, \quad \langle x^{-1} \rangle_{\bar{K}} = 3.42, \tag{45}$$

and the inverse moment of vector mesons' light-cone distribution amplitudes are obtained utilizing the Gegenbauer moments evaluated in QCD sum rules [38]:

$$\langle x^{-1} \rangle_\rho = \langle x^{-1} \rangle_\omega = 3.45, \quad \langle x^{-1} \rangle_\phi = 3.54,$$
$$\langle x^{-1} \rangle_{K^*} = 2.79, \quad \langle x^{-1} \rangle_{\bar{K}^*} = 3.81. \tag{46}$$

For the chiral scale parameters, we use a universal value $\mu_P = 2.0$ GeV for pseudoscalars and $\mu_V = 0$ for vectors.

The experimental data of $B \to PP$ and $B \to VP$ branching ratios, the direct CP asymmetries, and the parameters in $B^0/\bar{B}^0 \to \pi^\pm \rho^\mp$ decays [which are defined in Eqs. (73)–(75)] are given by the Heavy Flavor Averaging Group (HFAG) [39] and Particle Data Group (PDG) [40]. The following mixing-induced CP asymmetries in $B \to PP$ and $B \to VP$ decays are also used in our analysis:

$$-\eta_f S(K_S \eta') = 0.61 \pm 0.07,$$
$$-\eta_f S(K_S \pi^0) = 0.38 \pm 0.19,$$
$$S(\pi^+ \pi^-) = -0.61 \pm 0.08,$$
$$-\eta_f S(\phi K_S) = 0.39 \pm 0.17,$$
$$S(\pi^0 \rho^0) = 0.12 \pm 0.38,$$
$$-\eta_f S(\rho^0 K_S) = 0.61^{+0.22}_{-0.24} \pm 0.09 \pm 0.08 = 0.61^{+0.25}_{-0.27},$$
$$-\eta_f S(\omega K_S) = 0.48 \pm 0.24, \tag{47}$$

where η_f is the CP eigenvalue for the final state f. The branching ratio of $\bar{B}^0 \to \bar{K}^{*0} \pi^0$ is not used in this fitting, since the experimental data could only be viewed as an upper bound.

With these data for branching fractions and CP asymmetries, the χ^2 fit method is used to determine the nonperturbative inputs: form factors and charming penguins. Straightforwardly, we obtain the two solutions for numerical results of the 16 nonperturbative inputs. At leading order and leading power accuracy, the first solution is (the charming penguins are given in units of GeV)

$$\zeta^P = (12.8 \pm 1.2) \times 10^{-2},$$
$$\zeta_J^P = (7.2 \pm 0.7) \times 10^{-2},$$
$$\zeta^V = (12.4 \pm 1.8) \times 10^{-2},$$
$$\zeta_J^V = (10.8 \pm 1.9) \times 10^{-2},$$
$$\zeta_g = (-5.3 \pm 2.2) \times 10^{-2},$$
$$\zeta_{Jg} = (-2.3 \pm 2.9) \times 10^{-2},$$
$$|A_{cc}^{PP}| = (48.1 \pm 0.6) \times 10^{-4},$$
$$\arg[A_{cc}^{PP}] = (167.5 \pm 2.5)°,$$
$$|A_{cc}^{VP}| = (40.6 \pm 0.9) \times 10^{-4},$$
$$\arg[A_{cc}^{VP}] = (10.7 \pm 4.3)°,$$
$$|A_{cc}^{PV}| = (30.7 \pm 1.3) \times 10^{-4},$$
$$\arg[A_{cc}^{PV}] = (194.3 \pm 4.6)°,$$
$$|A_{ccg}^{PP}| = (38.4 \pm 1.9) \times 10^{-4},$$
$$\arg[A_{ccg}^{PP}] = (83.0 \pm 3.8)°,$$
$$|A_{ccg}^{VP}| = (23.0 \pm 2.4) \times 10^{-4},$$
$$\arg[A_{ccg}^{VP}] = (38.4 \pm 23.0)°, \tag{48}$$

and one can obtain the predictions for $B \to P$ (here P denotes a pseudoscalar except η and η') and $B \to V$ form factors at tree level:

$$F^{B \to P} = \zeta^P + \zeta_J^P = 0.201 \pm 0.015,$$
$$A_0^{B \to V} = \zeta^V + \zeta_J^V = 0.232 \pm 0.037. \tag{49}$$

In the above equations (and also in the following), the uncertainties are obtained through the χ^2-fit program. After including the chirally enhanced penguin, the numerical results for these inputs are (the charming penguins are given in units of GeV)

$$\begin{aligned}
\zeta^P &= (13.7 \pm 0.8) \times 10^{-2}, \\
\zeta_J^P &= (6.9 \pm 0.7) \times 10^{-2}, \\
\zeta^V &= (11.7 \pm 1.0) \times 10^{-2}, \\
\zeta_J^V &= (11.6 \pm 0.9) \times 10^{-2}, \\
\zeta_g &= (-4.9 \pm 2.4) \times 10^{-2}, \\
\zeta_{Jg} &= (-2.7 \pm 3.2) \times 10^{-2}, \\
|A_{cc}^{PP}| &= (40.0 \pm 0.6) \times 10^{-4}, \\
\arg[A_{cc}^{PP}] &= (165.2 \pm 2.8)^\circ, \\
|A_{cc}^{VP}| &= (41.0 \pm 0.9) \times 10^{-4}, \\
\arg[A_{cc}^{VP}] &= (11.9 \pm 4.2)^\circ, \\
|A_{cc}^{PV}| &= (39.9 \pm 1.0) \times 10^{-4}, \\
\arg[A_{cc}^{PV}] &= (191.5 \pm 3.6)^\circ, \\
|A_{ccg}^{PP}| &= (37.7 \pm 1.8) \times 10^{-4}, \\
\arg[A_{ccg}^{PP}] &= (88.3 \pm 4.1)^\circ, \\
|A_{ccg}^{VP}| &= (25.3 \pm 2.3) \times 10^{-4}, \\
\arg[A_{ccg}^{VP}] &= (-18.7 \pm 12.3)^\circ,
\end{aligned} \tag{50}$$

which gives the predictions for $B \to P$ and $B \to V$ form factors at tree level:

$$F^{B\to P} = 0.206 \pm 0.004, \qquad A_0^{B\to V} = 0.233 \pm 0.017. \tag{51}$$

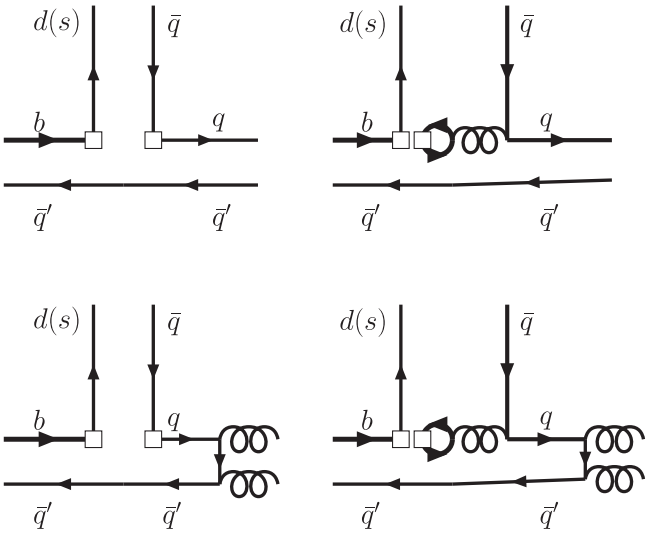

FIG. 1. Feynman diagrams for chiraly enhanced penguins (left) and charming penguins (right). The two diagrams in the lower line only contribute to decays involving η or η', where $q = q'$.

As shown in Fig. 1, chirally enhanced penguins have the same topology with the charming penguins. The former two diagrams do not only contribute to decays without isosinglet mesons η or η' but also decays with these mesons. The two diagrams in the lower line only contribute to decays involving η or η', where $q = q'$. The inclusion of a chirally enhanced penguin will mainly change the size of three charming penguins $A_{cc}^{PP}, A_{ccg}^{PP}, A_{cc}^{PV}$. Predictions for branching fractions and CP asymmetries will not be changed sizably. After including the chirally enhanced penguins, the total χ^2/d.o.f for observables $B \to PP$ and $B \to VP$ is $301/(86-16)$. If only the 55 observables in $B \to VP$ decays are concerned, the total χ^2 is 112.

Besides the above results, there is another solution at leading power:

$$\begin{aligned}
\zeta^P &= (13.4 \pm 0.3) \times 10^{-2}, \\
\zeta_J^P &= (5.8 \pm 0.4) \times 10^{-2}, \\
\zeta^V &= (22.9 \pm 1.3) \times 10^{-2}, \\
\zeta_J^V &= (6.6 \pm 1.4) \times 10^{-2}, \\
\zeta_g &= (-10.3 \pm 1.2) \times 10^{-2}, \\
\zeta_{Jg} &= (5.8 \pm 1.5) \times 10^{-2}, \\
|A_{cc}^{PP}| &= (48.4 \pm 0.4) \times 10^{-4}, \\
\arg[A_{cc}^{PP}] &= (167.1 \pm 2.6)^\circ, \\
|A_{cc}^{VP}| &= (29.7 \pm 0.8) \times 10^{-4}, \\
\arg[A_{cc}^{VP}] &= (159.3 \pm 6.9)^\circ, \\
|A_{cc}^{PV}| &= (44.9 \pm 1.1) \times 10^{-4}, \\
\arg[A_{cc}^{PV}] &= (-10.5 \pm 2.9)^\circ, \\
|A_{ccg}^{PP}| &= (38.4 \pm 2.2) \times 10^{-4}, \\
\arg[A_{ccg}^{PP}] &= (83.8 \pm 4.5)^\circ, \\
|A_{ccg}^{VP}| &= (18.6 \pm 2.3) \times 10^{-4}, \\
\arg[A_{ccg}^{VP}] &= (220.6 \pm 10.7)^\circ,
\end{aligned} \tag{52}$$

which gives

$$F^{B\to P} = 0.192 \pm 0.005, \qquad A_0^{B\to V} = 0.295 \pm 0.009. \tag{53}$$

With the inclusion of a chirally enhanced penguin, these inputs become

$$\begin{aligned}
\zeta^P &= (14.1 \pm 0.8) \times 10^{-2}, \\
\zeta^P_J &= (5.6 \pm 0.7) \times 10^{-2}, \\
\zeta^V &= (22.7 \pm 1.7) \times 10^{-2}, \\
\zeta^V_J &= (6.5 \pm 1.8) \times 10^{-2}, \\
\zeta_g &= (-10.0 \pm 0.9) \times 10^{-2}, \\
\zeta_{Jg} &= (5.1 \pm 1.1) \times 10^{-2}, \\
|A^{PP}_{cc}| &= (40.6 \pm 0.6) \times 10^{-4}, \\
\arg[A^{PP}_{cc}] &= (164.9 \pm 2.8)^\circ, \\
|A^{VP}_{cc}| &= (29.4 \pm 0.8) \times 10^{-4}, \\
\arg[A^{VP}_{cc}] &= (158.4 \pm 5.8)^\circ, \\
|A^{PV}_{cc}| &= (33.5 \pm 1.1) \times 10^{-4}, \\
\arg[A^{PV}_{cc}] &= (-14.3 \pm 3.8)^\circ, \\
|A^{PP}_{ccg}| &= (37.8 \pm 1.3) \times 10^{-4}, \\
\arg[A^{PP}_{ccg}] &= (87.5 \pm 2.1)^\circ, \\
|A^{VP}_{ccg}| &= (18.3 \pm 2.4) \times 10^{-4}, \\
\arg[A^{VP}_{ccg}] &= (225.6 \pm 10.0)^\circ,
\end{aligned} \tag{54}$$

with the form factors

$$F^{B\to P} = 0.198 \pm 0.003, \qquad A_0^{B\to V} = 0.291 \pm 0.011. \tag{55}$$

The corresponding $\chi^2 = 271/(86-16)$ (χ^2 for the 55 observables in all $B \to VP$ decays is 69). Comparing the results in the leading order analysis and those with chirally enhanced penguins, we can see that the charming penguins A^{PP}_{cc} and A^{PV}_{cc} are changed sizably. It is reasonable since chirally enhanced penguins and charming penguins have the same topology. The phase of A^{VP}_{ccg} is also changed sizably. It implies that the total statistical significance χ^2 is not very sensitive to $\arg[A^{VP}_{ccg}]$. The large error in this parameter also confirms this feature.

Using the two solutions for these nonperturbative inputs, we obtain two different kinds of predictions (labeled as This work 1 and This work 2) on branching fractions and CP asymmetries, where the chirally enhanced penguins are taken into account. As we have shown in the above, the leading power results are not very different from these results, as the inclusion of chirally enhanced penguins only amounts to a redefinition of charming penguins. Results for CP-averaged branching fractions are summarized in Tables I, III, and V, while predictions on direct CP asymmetries are given in Tables II, IV, and VI. In $B^0/\bar{B}^0 \to \pi^\mp\rho^\pm$ decays, it is easy to identify the final state mesons. Thus one can sum $B^0/\bar{B}^0 \to \pi^-\rho^+$ up as one channel, although the summed channels are not CP conjugates. The $B^0/\bar{B}^0 \to \pi^+\rho^-$ can be summed as another channel and it is also similar for the branching ratios of $B^0/\bar{B}^0 \to K^*K$ and $B^0_s/\bar{B}^0_s \to K^*K$ decays. In Tables I and V, we give our predictions on the summed branching ratios in $B^0/\bar{B}^0 \to \pi^\mp\rho^\pm$, $K^{*0}\bar{K}^0(\bar{K}^{*0}K^0)$ and two $B_s \to K^*K$ decays. We also give the predictions on the sum of the CP-averaged branching ratios of $\bar{B}^0 \to \pi^-\rho^+$ and $\bar{B}^0 \to \pi^+\rho^-$ and the other three $B_{(s)}$ decays in Tables I and VI. In order to compare with the QCDF approach [10,49–53] and PQCD approach [41–44,46–48,54–59], we also collect their results in these tables, together with the experimental data available at HFAG [39].

Because several approximations are made in this work, there are some important possible corrections which we would like to address. First of all, our results for the 16 inputs are obtained through the exact flavor SU(3) symmetry for the form factors and charming penguins. The amplitudes may receive sizable corrections from the SU(3) symmetry breaking effect proportional to $m_s/\Lambda_{\rm QCD} \sim 0.3$. Second, since we have concentrated on the leading order analysis, the radiative corrections proportional to $\alpha_s(\sqrt{m_b\Lambda_{\rm QCD}})/\pi \sim 0.1$ are also neglected. Although we have included one of the most important power corrections (chirally enhanced penguins), the other parts of power corrections proportional to $\lambda = \sqrt{\Lambda_{\rm QCD}/m_b} \sim 0.3$ are not incorporated in our analysis. At last, there are also uncertainties from the input parameters such as the b quark mass, Wilson coefficients, etc. To characterize these effects, we vary the magnitudes of the nonperturbative charming penguins by 20% and the phases by 20°. We also assume that the gluonic form factors ζ_g and ζ_{Jg} have additional uncertainties (± 0.05). In the predictions for branching fractions and CP asymmetries collected in Tables I, II, III, IV, V, and VI, the first kinds of uncertainties are from these hadronic uncertainties: charming penguins and gluonic form factors; the second kinds of uncertainties are from those in the CKM matrix elements.

B. $b \to d$ transitions without $\eta^{(\prime)}$

$b \to d$ transitions are induced by the operators whose CKM matrix elements are $V_{ub}V^*_{id}(i = u, c, t)$. To make it clear, we decompose the decay amplitudes into three terms according to the CKM matrix elements:

$$\begin{aligned}
A(B \to M_1M_2) = \frac{G_F}{\sqrt{2}} m_B^2 \{ & V_{ub}V^*_{ud}A_u + V_{cb}V^*_{cd}A_c \\
& - V_{tb}V^*_{td}A_t\},
\end{aligned} \tag{56}$$

where A_c is from the charming penguin term. The decomposition is over complete since the unitarity property of the CKM matrix can be used to eliminate one of the three combinations of CKM matrix elements. We keep all of them according to the different dynamics in the corresponding amplitudes. The values for CKM matrix elements,

TABLE I. Branching ratios (in units of 10^{-6}) of $B \to VP$ decays induced by the $b \to d$ ($\Delta S = 0$) transition: the first solution (This work 1) and the second solution (This work 2). In both cases, we have included the chirally enhanced penguin in $B \to VP$ decay amplitudes. The first kind of uncertainties are from uncertainties in charming penguins and gluonic form factors as discussed in the text; the second kind of uncertainties are from those in the CKM matrix elements. We also cite the experimental data and theoretical results given in QCDF [10] and PQCD [41–44] approaches to make a comparison.

Channel	Exp.	QCDF	PQCD	This work 1	This work 2
$B^- \to \rho^- \pi^0$	$10.9^{+1.4}_{-1.5}$	$14.0^{+6.5+5.1+1.0+0.8}_{-5.5-4.3-0.6-0.7}$	6–9	$8.9^{+0.3+1.0}_{-0.1-1.0}$	$11.4^{+0.6+1.1}_{-0.6-0.9}$
$B^- \to \rho^0 \pi^-$	$8.7^{+1.0}_{-1.1}$	$11.9^{+6.3+3.6+2.5+1.3}_{-5.0-3.1-1.2-1.1}$	$10.4^{+3.3}_{-3.4} \pm 2.1$	$10.7^{+0.7+1.0}_{-0.7-0.9}$	$7.9^{+0.2+0.8}_{-0.1-0.8}$
$B^- \to \omega \pi^-$	6.9 ± 0.5	$8.8^{+4.4+2.6+1.8+0.8}_{-3.5-2.2-0.9-0.9}$	$11.3^{+3.3}_{-2.9} \pm 1.4$	$6.7^{+0.4+0.7}_{-0.3-0.6}$	$8.5^{+0.3+0.8}_{-0.3-0.8}$
$B^- \to K^{*0} K^-$	<1.1	$0.30^{+0.11+0.12+0.09+0.57}_{-0.09-0.10-0.09-0.19}$	$0.31^{+0.12}_{-0.08}$	$0.49^{+0.26+0.09}_{-0.20-0.08}$	$0.51^{+0.18+0.07}_{-0.16-0.06}$
$B^- \to K^{*-} K^0$		$0.30^{+0.08+0.41+0.08+0.58}_{-0.07-0.18-0.07-0.17}$	$1.83^{+0.68}_{-0.47}$	$0.54^{+0.26+0.10}_{-0.21-0.08}$	$0.51^{+0.21+0.08}_{-0.17-0.07}$
$B^- \to \phi \pi^-$	<0.24	≈ 0.005		≈ 0.003	≈ 0.003
$\bar{B}^0 \to \rho^- \pi^+$ $\bar{B}^0 \to \rho^+ \pi^-$	24.0 ± 2.5	$36.5^{+18.2+10.3+2.0+3.9}_{-14.7-8.6-3.5-2.9}$	18–45	$13.4^{+0.6+1.2}_{-0.5-1.2}$	$16.8^{+0.5+1.6}_{-0.5-1.5}$
$B^0/\bar{B}^0 \to \rho^+ \pi^-$			24–34	$12.0^{+1.9+1.2}_{-1.6-1.1}$	$14.8^{+1.6+1.5}_{-1.5-1.4}$
$B^0/\bar{B}^0 \to \rho^- \pi^+$			24–34	$14.9^{+1.9+1.3}_{-1.9-1.3}$	$18.7^{+1.5+1.7}_{-1.6-1.6}$
$\bar{B}^0 \to \rho^+ \pi^-$ [a]	8.9 ± 2.5	$15.4^{+8.0+5.5+0.7+1.9}_{-6.4-4.7-1.3-1.3}$		$5.9^{+0.5+0.5}_{-0.5-0.5}$	$6.6^{+0.2+0.7}_{-0.1-0.7}$
$\bar{B}^0 \to \rho^- \pi^+$ [a]	13.9 ± 2.7	$21.2^{+10.3+8.7+1.3+2.0}_{-8.4-7.2-2.3-1.6}$		$7.5^{+0.3+0.8}_{-0.1-0.8}$	$10.2^{+0.4+0.9}_{-0.5-0.9}$
$\bar{B}^0 \to \rho^0 \pi^0$	$1.8^{+0.6}_{-0.5}$	$0.4^{+0.2+0.2+0.9+0.5}_{-0.2-0.1-0.3-0.3}$	0.07–0.11	$2.5^{+0.2+0.2}_{-0.1-0.2}$	$1.5^{+0.1+0.1}_{-0.1-0.1}$
$\bar{B}^0 \to \omega \pi^0$	<1.2	$0.01^{+0.00+0.02+0.02+0.03}_{-0.00-0.00-0.00-0.00}$	0.10–2.28	$0.0003^{+0.0299+0.0000}_{-0.0000-0.0000}$	$0.015^{+0.024+0.002}_{-0.000-0.002}$
$\bar{B}^0 \to K^{*0} \bar{K}^0$		$0.26^{+0.08+0.10+0.08+0.46}_{-0.07-0.09-0.08-0.15}$		$0.45^{+0.24+0.09}_{-0.19-0.07}$	$0.47^{+0.17+0.06}_{-0.14-0.05}$
$\bar{B}^0 \to \bar{K}^{*0} K^0$	<1.9	$0.29^{+0.10+0.39+0.08+0.60}_{-0.09-0.17-0.07-0.17}$		$0.51^{+0.24+0.09}_{-0.20-0.08}$	$0.48^{+0.20+0.07}_{-0.16-0.06}$
$\bar{B}^0 \to K^{*0} \bar{K}^0$ $\bar{B}^0 \to \bar{K}^{*0} K^0$			≈ 1.96	$0.96^{+0.34+0.18}_{-0.27-0.15}$	$0.95^{+0.26+0.14}_{-0.22-0.12}$
$B^0/\bar{B}^0 \to K^{*0} \bar{K}^0$				$0.95^{+0.34+0.18}_{-0.27-0.15}$	$0.94^{+0.26+0.14}_{-0.22-0.12}$
$B^0/\bar{B}^0 \to \bar{K}^{*0} K^0$				$0.97^{+0.35+0.18}_{-0.27-0.15}$	$0.97^{+0.26+0.14}_{-0.22-0.12}$
$\bar{B}^0 \to \phi \pi^0$	<0.28	≈ 0.002		≈ 0.001	≈ 0.001
$B^- \to \rho^- \eta$	5.4 ± 1.2	$9.4^{+4.6+3.6+0.7+0.7}_{-3.7-3.0-0.4-0.7}$	$8.5^{+3.0+0.8+0.4+1.2}_{-2.1-0.7-0.4-0.2}$ [b]	$3.9^{+2.0+0.4}_{-1.7-0.4}$	$3.3^{+1.9+0.3}_{-1.6-0.3}$
$B^- \to \rho^- \eta'$	$9.1^{+3.7}_{-2.8}$	$6.3^{+3.1+2.4+0.5+0.5}_{-2.5-2.0-0.3-0.5}$	$8.7^{+3.0+0.7+0.5+1.1}_{-2.2-0.9-0.7-0.3}$ [b]	$0.37^{+2.46+0.08}_{-0.22-0.07}$	$0.44^{+3.18+0.06}_{-0.20-0.05}$
$\bar{B}^0 \to \rho^0 \eta$	<1.5	$0.03^{+0.02+0.16+0.02+0.05}_{-0.01-0.10-0.01-0.02}$	$0.024^{+0.012+0.004+0.002+0.102}_{-0.007-0.002-0.002-0.005}$ [b]	$0.04^{+0.20+0.00}_{-0.01-0.00}$	$0.14^{+0.33+0.01}_{-0.13-0.01}$
$\bar{B}^0 \to \rho^0 \eta'$	<1.3	$0.01^{+0.01+0.11+0.02+0.03}_{-0.00-0.06-0.00-0.01}$	$0.061^{+0.030+0.004+0.003+0.114}_{-0.018-0.003-0.003-0.009}$ [b]	$0.43^{+2.51+0.05}_{-0.12-0.05}$	$1.0^{+3.5+0.1}_{-0.9-0.1}$
$\bar{B}^0 \to \omega \eta$	<1.9	$0.31^{+0.14+0.16+0.35+0.22}_{-0.12-0.11-0.14-0.16}$	$0.27^{+0.11}_{-0.10}$	$0.91^{+0.66+0.09}_{-0.49-0.09}$	$1.4^{+0.8+0.1}_{-0.6-0.1}$
$\bar{B}^0 \to \omega \eta'$	<2.2	$0.20^{+0.10+0.15+0.25+0.15}_{-0.08-0.05-0.10-0.11}$	$0.075^{+0.037}_{-0.033}$	$0.18^{+1.31+0.04}_{-0.10-0.03}$	$3.1^{+4.9+0.3}_{-2.6-0.3}$
$\bar{B}^0 \to \phi \eta$	<0.6	≈ 0.001	$0.0063^{+0.0033}_{-0.0019}$	≈ 0.0004	≈ 0.0008
$\bar{B}^0 \to \phi \eta'$	<0.5	≈ 0.001	$0.0073^{+0.0035}_{-0.0026}$	≈ 0.0001	≈ 0.0007

[a] We quote the branching ratios for $\bar{B}^0 \to \rho^+ \pi^-$ and $\bar{B}^0 \to \rho^+ \pi^-$ from Ref. [45].
[b] For $B \to \rho \eta$ decays, there are two different predictions given in Ref. [42] according to the different mixing angles between η and η'. We quote the results in which $\theta_P = -10°$ is used. There are not too many changes for the other predictions as the value for the mixing angle $\theta_P = -17°$ is very close to the first one.

$$
\begin{aligned}
|V_{ub} V_{ud}^*| &= 3.48 \times 10^{-3}, \\
|V_{cb} V_{cd}^*| &= 9.17 \times 10^{-3}, \\
|V_{tb} V_{td}^*| &= 8.60 \times 10^{-3}
\end{aligned} \tag{57}
$$

will definitely characterize the branching fractions and CP asymmetries.

$\bar{B}^0 \to \pi^\pm \rho^\mp$ are dominated by tree operators which have the CKM matrix elements: $V_{ub} V_{ud}^*$. To illustrate the situation, we will use the second kind of inputs given in Eq. (54) and take $\bar{B}^0 \to \rho^+ \pi^-$ as an example (in units of GeV):

$$
\begin{aligned}
|A_u(\bar{B}^0 \to \rho^+ \pi^-)| &= 0.131 \times (1.03 \zeta^V + 0.77 \zeta_J^V) \\
&\sim 260 \times 10^{-4}, \\
|A_c(\bar{B}^0 \to \rho^+ \pi^-)| &= |A_{cc}^{PV}| \sim (30 \sim 40) \times 10^{-4}, \\
|A_t(\bar{B}^0 \to \rho^+ \pi^-)| &= |0.131(-0.0015 \zeta^V - 0.007 \zeta_J^V)| \\
&\sim 5 \times 10^{-4}.
\end{aligned} \tag{58}
$$

Our predictions on branching fractions of $\bar{B}^0 \to \pi^\pm \rho^\mp$

TABLE II. Direct CP asymmetries involving $b \to d$ ($\Delta S = 0$) transitions: the first solution (This work 1) and the second solution (This work 2). In both solutions, we have included the chirally enhanced penguin in $B \to VP$ decay amplitudes. The first kind of uncertainties are from uncertainties in charming penguins and gluonic form factors which are discussed in the text; the second kind of uncertainties are from those in the CKM matrix elements. We also cite the experimental data and theoretical results given in QCDF [10] and PQCD [41–44] approaches to make a comparison.

Channel	Exp.	QCDF	PQCD	This work 1	This work 2
$B^- \to \rho^- \pi^0$	2 ± 11	$-4.0^{+1.2+1.8+0.4+17.5}_{-1.2-2.2-0.4-17.7}$	0–20	$15.5^{+16.9+1.6}_{-18.9-1.4}$	$12.3^{+9.4+0.9}_{-10.0-1.1}$
$B^- \to \rho^0 \pi^-$	-7^{+12}_{-13}	$4.1^{+1.3+2.2+0.6+19.0}_{-0.9-2.0-0.7-18.8}$	$-20- - 0$	$-10.8^{+13.1+0.9}_{-12.7-0.7}$	$-19.2^{+15.5+1.7}_{-13.4-1.9}$
$B^- \to \omega \pi^-$	-4 ± 6	$-1.8^{+0.5+2.7+0.8+2.1}_{-0.5-3.3-0.7-2.2}$	~ 0	$0.5^{+19.1+0.1}_{-19.6-0.0}$	$2.3^{+13.4+0.2}_{-13.2-0.2}$
$B^- \to K^{*0} K^-$	$\ldots$	$-23.5^{+6.9+7.8+5.5+25.2}_{-5.7-9.0-6.5-36.8}$	$-20 \pm 5 \pm 2$	$-3.6^{+6.1+0.4}_{-5.3-0.4}$	$-4.4^{+4.1+0.2}_{-4.1-0.2}$
$B^- \to K^{*-} K^0$	$\ldots$	$-13.4^{+3.7+7.8+4.2+27.4}_{-3.0-3.5-4.7-36.7}$	-49^{+7+7}_{-3-7}	$-1.5^{+2.6+0.1}_{-2.3-0.1}$	$-1.2^{+1.7+0.1}_{-1.7-0.1}$
$\bar{B}^0 \to \rho^+ \pi^-$	-18 ± 12	$0.6^{+0.2+1.3+0.1+11.5}_{-0.1-1.6-0.1-11.7}$		$-9.9^{+17.2+0.9}_{-16.7-0.7}$	$-12.4^{+17.6+1.1}_{-15.3-1.2}$
$\bar{B}^0 \to \rho^- \pi^+$	11 ± 6	$-1.5^{+0.4+1.2+0.2+8.5}_{-0.4-1.3-0.3-8.4}$		$11.8^{+17.5+1.2}_{-20.0-1.1}$	$10.8^{+9.4+0.9}_{-10.2-1.0}$
$\bar{B}^0 \to \rho^0 \pi^0$	-30 ± 38	$-15.7^{+4.8+12.3+11.0+19.8}_{-4.7-14.0-12.9-25.8}$	$-75 - 0$	$-0.6^{+21.4+0.1}_{-21.9-0.1}$	$-3.5^{+21.4+0.3}_{-20.3-0.3}$
$\bar{B}^0 \to \omega \pi^0$	$\ldots$	$\ldots$	-20–75	$-9.4^{+24.0+1.1}_{-0.0-0.9}$	$39.5^{+79.1+3.4}_{-185.5-3.1}$
$\bar{B}^0 \to K^{*0} \bar{K}^0$	$\ldots$	$-26.7^{+7.4+7.2+5.7+10.9}_{-5.7-9.0-6.9-13.4}$		$-3.6^{+6.1+0.4}_{-5.3-0.4}$	$-4.4^{+4.1+0.2}_{-4.1-0.2}$
$\bar{B}^0 \to \bar{K}^{*0} K^0$	$\ldots$	$-13.1^{+3.8+5.4+4.5+5.8}_{-3.0-2.9-5.2-7.4}$		$-1.5^{+2.6+0.1}_{-2.3-0.1}$	$-1.2^{+1.7+0.1}_{-1.7-0.1}$
$B^- \to \rho^- \eta$	1 ± 16	$-2.4^{+0.7+6.3+0.4+0.2}_{-0.7-6.3-0.4-0.2}$	$-13^{+1.2+2}_{-0.5-14}$	$-6.6^{+21.5+0.6}_{-21.3-0.7}$	$-9.1^{+16.7+0.9}_{-15.8-0.8}$
$B^- \to \rho^- \eta'$	-4 ± 28	$4.1^{+1.2+7.9+0.5+7.0}_{-1.1-6.9-0.8-7.0}$	$-18^{+3.0+1}_{-1.6-14}$	$-19.8^{+66.5+2.8}_{-37.5-3.1}$	$-21.7^{+135.9+2.1}_{-24.3-1.7}$
$\bar{B}^0 \to \rho^0 \eta$	$\ldots$	$\ldots$	$-13^{+1.2+2}_{-0.5-14}$	$-46.7^{+170.4+2.9}_{-74.3-3.7}$	$33.3^{+66.9+3.1}_{-62.4-2.8}$
$\bar{B}^0 \to \rho^0 \eta'$	$\ldots$	$\ldots$	$-18^{+3.0+1}_{-1.6-14}$	$-51.7^{+103.3+3.4}_{-42.9-3.9}$	$52.2^{+19.9+4.4}_{-80.6-4.1}$
$\bar{B}^0 \to \omega \eta$	$\ldots$	$-33.4^{+10.0+65.3+20.9+19.2}_{-9.5-55.8-21.4-20.8}$	$-69.1^{+15.1}_{-13.4}$	$-9.4^{+30.7+0.9}_{-30.2-1.0}$	$-9.6^{+17.8+0.9}_{-16.8-0.9}$
$\bar{B}^0 \to \omega \eta'$	$\ldots$	$0.2^{+0.1+53.0+11.6+19.2}_{-0.1-76.5-11.5-20.1}$	$13.9^{+4.1}_{-3.5}$	$-43.0^{+87.5+4.8}_{-38.8-5.1}$	$-27.2^{+18.1+2.4}_{-29.7-2.2}$

TABLE III. Branching ratios (in units of 10^{-6}) for $\Delta s = 1$ processes: the first solution (This work 1) and the second solution (This work 2). In both solutions, we have included the chirally enhanced penguin in $B \to VP$ decay amplitudes. The first kind of uncertainties are from uncertainties in charming penguins and gluonic form factors which are discussed in the text; the second kind of uncertainties are from those in the CKM matrix elements. We also cite the experimental data and theoretical results given in QCDF [10] and PQCD [46,47] to make a comparison.

Channel	Exp.	QCDF	PQCD	This work 1	This work 2
$B^- \to K^{*-} \pi^0$	6.9 ± 2.3	$3.3^{+1.1+1.0+0.6+4.4}_{-1.0-0.9-0.6-1.4}$	$4.3^{+5.0}_{-2.2}$	$4.2^{+2.2+0.8}_{-1.7-0.7}$	$6.5^{+1.9+0.7}_{-1.7-0.7}$
$B^- \to \bar{K}^{*0} \pi^-$	10.7 ± 0.8	$3.6^{+0.4+1.5+1.2+7.7}_{-0.3-1.4-1.2-2.3}$	$6.0^{+2.8}_{-1.5}$	$8.5^{+4.7+1.7}_{-3.6-1.4}$	$9.9^{+3.5+1.3}_{-3.0-1.1}$
$B^- \to \rho^0 K^-$	$4.25^{+0.55}_{-0.56}$	$2.6^{+0.9+3.1+0.8+4.3}_{-0.9-1.4-0.6-1.2}$	$5.1^{+4.1}_{-2.8}$	$6.7^{+2.7+1.0}_{-2.2-0.9}$	$4.6^{+1.8+0.7}_{-1.5-0.6}$
$B^- \to \rho^- \bar{K}^0$	$8.0^{+1.5}_{-1.4}$	$5.8^{+0.6+7.0+1.5+10.3}_{-0.6-3.3-1.3-3.2}$	$8.7^{+6.8}_{-4.4}$	$9.3^{+4.7+1.7}_{-3.7-1.4}$	$10.1^{+4.0+1.5}_{-3.3-1.3}$
$B^- \to \omega K^-$	6.7 ± 0.5	$3.5^{+1.0+3.3+1.4+4.7}_{-1.0-1.6-0.9-1.6}$	$10.6^{+10.4}_{-5.8}$	$5.1^{+2.4+0.9}_{-1.9-0.8}$	$5.9^{+2.1+0.8}_{-1.7-0.7}$
$B^- \to \phi K^-$	8.30 ± 0.65	$4.5^{+0.5+1.8+1.9+11.8}_{-0.4-1.7-2.1-3.3}$	$7.8^{+5.9}_{-1.8}$	$9.7^{+4.9+1.8}_{-3.9-1.5}$	$8.6^{+3.2+1.2}_{-2.7-1.0}$
$\bar{B}^0 \to \bar{K}^{*0} \pi^0$	$0.0^{+1.3}_{-0.1}$	$0.7^{+0.1+0.5+0.3+2.6}_{-0.1-0.4-0.3-0.5}$	$2.0^{+1.2}_{-0.6}$	$4.6^{+2.3+0.9}_{-1.8-0.7}$	$3.7^{+1.4+0.5}_{-1.2-0.5}$
$\bar{B}^0 \to \bar{K}^{*-} \pi^+$	9.8 ± 1.1	$3.3^{+1.4+1.3+0.8+6.2}_{-1.1-1.2-0.8-1.6}$	$6.0^{+6.8}_{-2.6}$	$8.4^{+4.4+1.6}_{-3.4-1.3}$	$9.5^{+3.2+1.2}_{-2.8-1.1}$
$\bar{B}^0 \to \rho^0 \bar{K}^0$	$5.4^{+0.9}_{-1.0}$	$4.6^{+0.5+4.0+0.7+6.1}_{-0.5-2.1-0.7-2.1}$	$4.8^{+4.3}_{-2.3}$	$3.5^{+2.0+0.7}_{-1.5-0.6}$	$5.8^{+2.1+0.8}_{-1.8-0.7}$
$\bar{B}^0 \to \rho^+ K^-$	$15.3^{+3.7}_{-3.5}$	$7.4^{+1.8+7.1+1.2+10.7}_{-1.9-3.6-1.1-3.5}$	$8.8^{+6.8}_{-4.5}$	$9.8^{+4.6+1.7}_{-3.7-1.4}$	$10.2^{+3.8+1.5}_{-3.2-1.2}$
$\bar{B}^0 \to \omega \bar{K}^0$	5.0 ± 0.6	$2.3^{+0.3+2.8+1.3+4.3}_{-0.3-1.3-0.8-1.3}$	$9.8^{+8.6}_{-4.9}$	$4.1^{+2.1+0.8}_{-1.7-0.7}$	$4.9^{+1.9+0.7}_{-1.6-0.6}$
$\bar{B}^0 \to \phi \bar{K}^0$	$8.3^{+1.2}_{-1.0}$	$4.1^{+0.4+1.7+1.8+10.6}_{-0.4-1.6-1.9-3.0}$	$7.3^{+5.9}_{-1.8}$	$9.1^{+4.6+1.7}_{-3.6-1.4}$	$8.0^{+3.0+1.1}_{-2.5-1.0}$
$B^- \to K^{*-} \eta$	19.3 ± 1.6	$10.8^{+1.9+8.1+1.8+16.5}_{-1.7-4.4-1.3-5.5}$	$22.13^{+0.26}_{-0.27}$	$17.9^{+5.5+3.5}_{-5.4-2.9}$	$18.6^{+4.5+2.5}_{-4.8-2.2}$
$B^- \to K^{*-} \eta'$	$4.9^{+2.1}_{-1.9}$	$5.1^{+0.9+7.5+2.1+6.7}_{-1.0-3.8-3.0-3.3}$	6.38 ± 0.26	$4.5^{+6.6+0.9}_{-3.9-0.8}$	$4.8^{+5.3+0.8}_{-3.7-0.6}$
$\bar{B}^0 \to \bar{K}^{*0} \eta$	15.9 ± 1.0	$10.7^{+1.1+7.8+1.4+16.2}_{-1.0-4.3-1.2-5.5}$	$22.31^{+0.28}_{-0.29}$	$16.6^{+5.1+3.2}_{-5.0-2.7}$	$16.5^{+4.1+2.3}_{-4.3-2.0}$
$\bar{B}^0 \to \bar{K}^{*0} \eta'$	3.8 ± 1.2	$3.9^{+0.4+6.6+1.8+6.2}_{-0.4-3.3-2.5-2.9}$	$3.35^{+0.29}_{-0.27}$	$4.1^{+6.2+0.9}_{-3.6-0.7}$	$4.0^{+4.7+0.7}_{-3.4-0.6}$

TABLE IV. Direct CP asymmetries (in %) for $\Delta s = 1$ processes: the first solution (This work 1) and the second solution (This work 2). In both solutions, we have included the chirally enhanced penguin in $B \to VP$ decay amplitudes. The first kind of uncertainties are from uncertainties in charming penguins and gluonic form factors which are discussed in the text; the second kind of uncertainties are from those in the CKM matrix elements. We also cite the experimental data and theoretical results given in QCDF [10] and PQCD [46,47] to make a comparison.

Channel	Exp.	QCDF	PQCD	This work 1	This work 2
$B^- \to K^{*-}\pi^0$	4 ± 29	$8.7^{+2.1+5.0+2.9+41.7}_{-2.6-4.3-3.4-44.2}$	-32^{+21}_{-28}	$-17.8^{+30.3+2.2}_{-24.6-2.0}$	$-12.9^{+12.0+0.8}_{-12.2-0.8}$
$B^- \to \bar{K}^{*0}\pi^-$	-8.5 ± 5.7	$1.6^{+0.4+0.6+0.5+2.5}_{-0.5-0.5-0.4-1.0}$	-1^{+1}_{-0}	0	0
$B^- \to \rho^0 K^-$	31^{+11}_{-10}	$-13.6^{+4.5+6.9+3.7+62.7}_{-5.7-4.4-3.1-55.4}$	71^{+25}_{-35}	$9.2^{+15.2+0.7}_{-16.1-0.7}$	$16.0^{+20.5+1.3}_{-22.4-1.6}$
$B^- \to \rho^- \bar{K}^0$	-12 ± 17	$0.3^{+0.1+0.3+0.2+1.6}_{-0.1-0.4-0.1-1.3}$	1 ± 1	0	0
$B^- \to \omega K^-$	2 ± 5	$-7.8^{+2.6+5.9+2.4+39.8}_{-3.0-3.6-1.9-38.0}$	32^{+15}_{-17}	$11.6^{+18.2+1.1}_{-20.4-1.1}$	$12.3^{+16.6+0.8}_{-17.3-1.1}$
$B^- \to \phi K^-$	3.4 ± 4.4	$1.6^{+0.4+0.6+0.5+3.0}_{-0.5-0.5-0.3-1.2}$	1^{+0}_{-1}	0	0
$\bar{B}^0 \to \bar{K}^{*0}\pi^0$	...	$-12.8^{+4.0+4.7+2.7+31.7}_{-3.2-7.0-4.0-35.3}$	-11^{+7}_{-5}	$5.0^{+7.5+0.5}_{-8.4-0.5}$	$5.4^{+4.8+0.4}_{-5.1-0.5}$
$\bar{B}^0 \to \bar{K}^{*-}\pi^+$	-5 ± 14	$2.1^{+0.6+8.2+5.1+62.5}_{-0.7-7.9-5.8-64.2}$	-60^{+32}_{-19}	$-11.2^{+19.0+1.3}_{-16.2-1.3}$	$-12.2^{+11.4+0.8}_{-11.3-0.8}$
$\bar{B}^0 \to \rho^0 \bar{K}^0$	$-2 \pm 27 \pm 8 \pm 6$	$7.5^{+1.7+2.3+0.7+8.8}_{-2.1-2.0-0.4-8.7}$	7^{+8}_{-5}	$-6.6^{+11.6+0.8}_{-9.7-0.9}$	$-3.5^{+4.8+0.3}_{-4.8-0.2}$
$\bar{B}^0 \to \rho^+ K^-$	22 ± 23	$-3.8^{+1.3+4.4+1.9+34.5}_{-1.4-2.7-1.6-32.7}$	64^{+24}_{-30}	$7.1^{+11.2+0.7}_{-12.4-0.7}$	$9.6^{+13.0+0.7}_{-13.5-0.9}$
$\bar{B}^0 \to \omega \bar{K}^0$	21 ± 19	$-8.1^{+2.5+3.0+1.7+11.8}_{-2.0-3.3-1.4-12.9}$	-3^{+2}_{-3}	$5.2^{+8.0+0.6}_{-9.2-0.6}$	$3.8^{+5.2+0.3}_{-5.4-0.3}$
$\bar{B}^0 \to \phi \bar{K}^0$	1 ± 12	$1.7^{+0.4+0.6+0.5+1.4}_{-0.5-0.5-0.3-0.8}$	3^{+1}_{-2}	0	0
$B^- \to K^{*-}\eta$	2 ± 6	$3.5^{+0.9+1.9+0.8+20.7}_{-0.9-2.7-0.8-20.5}$	$-24.57^{+0.72}_{-0.27}$	$-2.6^{+5.4+0.3}_{-5.5-0.3}$	$-1.9^{+3.4+0.1}_{-3.6-0.1}$
$B^- \to K^{*-}\eta'$	30^{+33}_{-37}	$-14.2^{+4.7+8.5+4.9+27.5}_{-4.2-13.8-14.6-26.1}$	$4.60^{+1.16}_{-1.32}$	$2.7^{+27.4+0.4}_{-19.5-0.3}$	$2.6^{+26.7+0.2}_{-32.9-0.2}$
$\bar{B}^0 \to \bar{K}^{*0}\eta$	19 ± 5	$3.8^{+0.9+1.1+0.2+3.8}_{-1.1-0.8-0.2-3.5}$	0.57 ± 0.011	$-1.1^{+2.3+0.1}_{-2.4-0.1}$	$-0.7^{+1.2+0.1}_{-1.3-0.0}$
$\bar{B}^0 \to \bar{K}^{*0}\eta'$	-8 ± 25	$-5.5^{+1.6+3.1+1.8+6.2}_{-1.3-5.1-5.9-7.0}$	-1.30 ± 0.08	$9.6^{+8.9+1.3}_{-11.0-1.2}$	$9.9^{+6.2+0.9}_{-4.3-0.9}$

decays are smaller than those in QCDF [10]. Neglecting the small terms, the main reason is our smaller $B \to P$ and $B \to V$ form factors: QCDF uses much larger form factors $F^{B\to\pi} = 0.28 \pm 0.05$ and $A_0^{B\to\rho} = 0.37 \pm 0.06$. In the present framework, $\mathcal{BR}(\bar{B}^0 \to \rho^+\pi^-)$ is smaller than $\mathcal{BR}(\bar{B}^0 \to \rho^-\pi^+)$. In the first solution, the fitted $B \to V$ form factor $A_0 = 0.233$ is almost equal with the $B \to P$ form factor $F = 0.206$. Since the decay constant of the ρ meson is much larger than that of π, $0.209/0.131 \sim 1.5$, we expect $\mathcal{BR}(\bar{B}^0 \to \rho^+\pi^-)$ is only one half of $\mathcal{BR}(\bar{B}^0 \to \rho^-\pi^+)$. Charming penguins A_{cc}^{VP} and A_{cc}^{PV} can slightly change the ratio: the charming penguin A_{cc}^{PV} in $\bar{B}^0 \to \rho^+\pi^-$ gives a destructive contribution, while A_{cc}^{VP} in $\bar{B}^0 \to \rho^-\pi^+$ gives a constructive contribution. In the second solution, contributions proportional to form factors are almost equal with each other, as the $B \to V$ form factor $A_0^{B\to V} = 0.291$ is much larger than $F^{B\to P} = 0.198$ which can compensate differences caused by decay constants. But unlike in the first solution, the role of the charming penguin totally changes: the charming penguin in $\bar{B}^0 \to \rho^+\pi^-$ gives a constructive contribution, while A_{cc}^{VP} in $\bar{B}^0 \to \rho^-\pi^+$ can give a destructive contribution. It is reasonable, since the charming penguins A_{cc}^{VP} and A_{cc}^{PV} almost interchanges the phases.

Our predictions for branching ratios of $\bar{B}^0 \to \pi^0\rho^0$ are larger than that in QCDF especially the prediction utilizing the inputs given in Eq. (50). In this channel, two kinds of charming penguin almost cancel with each other, since they have similar magnitudes but different signs as given in Eqs. (50) and (54). The tree contribution proportional to the soft form factor ζ is color suppressed (the Wilson coefficient $C_2 + \frac{C_1}{N_c} \sim 0.12$ is small compared with that of $\bar{B}^0 \to \rho^\pm\pi^\mp$ $C_1 + \frac{C_2}{N_c} \sim 1.03$), thus the branching fractions of $\bar{B}^0 \to \pi^0\rho^0$ in the QCDF approach and PQCD approach are much smaller than $\mathcal{BR}(\bar{B}^0 \to \rho^\pm\pi^\mp)$. One important feature of the SCET framework is that the hard-scattering form factor ζ_J is relatively large and comparable with the soft form factor ζ. Besides, this term has a large Wilson coefficient b_1^f, since $C_2 + \frac{1}{N_c}(1 - \frac{m_b}{\omega_3})C_1 \sim 1.23$ is large, it can give larger production rates which are consistent with the present experimental data. The agreement is very encouraging.

Branching ratios of $B \to K^*K$ are larger than those in QCDF for the presence of charming penguins. In $B^- \to K^{*-}K^0$ and $\bar{B}^0 \to \bar{K}^{*0}K^0$, both penguin operators and charming penguins can give contributions. The difference for these two channels is that the spectator antiquark in $B^- \to K^{*-}K^0$ is $\bar{u}$ and it is $\bar{d}$ in $\bar{B}^0 \to \bar{K}^{*0}K^0$. It does not affect the contributions from either penguin operators or charming penguins, thus we expect the relations $\mathcal{BR}(B^- \to K^{*-}K^0) = \mathcal{BR}(\bar{B}^0 \to \bar{K}^{*0}K^0)$ and $A_{CP}(B^- \to K^{*-}K^0) = A_{CP}(\bar{B}^0 \to \bar{K}^{*0}K^0)$. The small differences in branching fractions are induced by the dif-

TABLE V. *CP*-averaged branching ratios ($\times 10^{-6}$) of $B_s \to PV$ decays: the first solution (This work 1) and the second solution (This work 2). In both solutions, we have included the chirally enhanced penguin in $B \to VP$ decay amplitudes. The first kind of uncertainties are from uncertainties in charming penguins and gluonic form factors which are discussed in the text; the second kind of uncertainties are from those in the CKM matrix elements. We also cite theoretical results evaluated in QCDF [10] and PQCD [48] to make a comparison.

Modes	QCDF	PQCD	This work 1	This work 2
$\bar{B}_s^0 \to K^+ K^{*-}$	$4.1^{+1.7+1.5+1.0+9.2}_{-1.5-1.3-0.9-2.3}$	$6.0^{+1.7+1.7+0.7}_{-1.5-1.2-0.3}$	$8.4^{+4.4+1.6}_{-3.4-1.3}$	$9.5^{+3.2+1.2}_{-2.8-1.1}$
$\bar{B}_s^0 \to K^{*+} K^-$	$5.5^{+1.3+5.0+0.8+14.2}_{-1.4-2.6-0.7-3.6}$	$4.7^{+1.1+2.5+0.0}_{-0.8-1.4-0.0}$	$9.8^{+4.6+1.7}_{-3.7-1.4}$	$10.2^{+3.8+1.5}_{-3.2-1.2}$
$\bar{B}_s^0 \to K^0 \bar{K}^{*0}$	$3.9^{+0.4+1.5+1.3+10.4}_{-0.4-1.4-1.4-2.8}$	$7.3^{+2.5+2.1+0.0}_{-1.7-1.3-0.0}$	$7.9^{+4.4+1.6}_{-3.4-1.3}$	$9.3^{+3.2+1.2}_{-2.8-1.0}$
$\bar{B}_s^0 \to K^{*0} \bar{K}^0$	$4.2^{+0.4+4.6+1.1+13.2}_{-0.4-2.2-0.9-3.2}$	$4.3^{+0.7+2.2+0.0}_{-0.7-1.4-0.0}$	$8.7^{+4.4+1.6}_{-3.5-1.4}$	$9.4^{+3.7+1.4}_{-3.1-1.2}$
$B_s^0/\bar{B}_s^0 \to K^+ K^{*-}$			$16.5^{+6.4+3.2}_{-4.9-2.6}$	$17.5^{+5.0+2.5}_{-4.4-2.1}$
$B_s^0/\bar{B}_s^0 \to K^{*+} K^-$			$19.8^{+6.9+3.4}_{-5.6-2.9}$	$21.8^{+5.4+2.8}_{-4.7-2.4}$
$\bar{B}_s^0 \to K^{*+} K^-$, $\bar{B}_s^0 \to K^{*-} K^+$			$18.2^{+6.3+3.3}_{-5.0-2.7}$	$19.7^{+5.0+2.6}_{-4.2-2.2}$
$\bar{B}_s^0 \to K^{*0} \bar{K}^0$, $\bar{B}_s^0 \to \bar{K}^{*0} K^0$			$16.6^{+6.2+3.2}_{-4.9-2.7}$	$18.7^{+4.9+2.6}_{-4.2-2.2}$
$\bar{B}_s^0 \to \pi^0 \phi$	$0.12^{+0.03+0.04+0.01+0.02}_{-0.02-0.04-0.01-0.01}$	$0.16^{+0.06+0.02+0.00}_{-0.05-0.02-0.00}$	$0.07^{+0.00+0.01}_{-0.00-0.01}$	$0.09^{+0.00+0.01}_{-0.00-0.01}$
$\bar{B}_s^0 \to \pi^- K^{*+}$	$8.7^{+4.6+3.5+0.7+0.8}_{-3.7-2.9-1.0-0.7}$	$7.6^{+2.9+0.4+0.5}_{-2.2-0.5-0.3}$	$5.9^{+0.5+0.5}_{-0.5-0.5}$	$6.6^{+0.2+0.7}_{-0.1-0.7}$
$\bar{B}_s^0 \to \pi^0 K^{*0}$	$0.25^{+0.08+0.10+0.32+0.30}_{-0.08-0.06-0.14-0.14}$	$0.07^{+0.02+0.04+0.01}_{-0.01-0.02-0.01}$	$0.90^{+0.07+0.10}_{-0.01-0.11}$	$1.07^{+0.16+0.10}_{-0.15-0.09}$
$\bar{B}_s^0 \to \rho^- K^+$	$24.5^{+11.9+9.2+1.8+1.6}_{-9.7-7.8-3.0-1.6}$	$17.8^{+7.7+1.3+1.1}_{-5.6-1.6-0.9}$	$7.6^{+0.3+0.8}_{-0.1-0.8}$	$10.2^{+0.4+0.9}_{-0.5-0.9}$
$\bar{B}_s^0 \to \rho^0 K^0$	$0.61^{+0.33+0.21+1.06+0.56}_{-0.26-0.15-0.38-0.36}$	$0.08^{+0.02+0.07+0.01}_{-0.02-0.03-0.00}$	$2.0^{+0.2+0.2}_{-0.2-0.2}$	$0.81^{+0.05+0.08}_{-0.02-0.09}$
$\bar{B}_s^0 \to K^0 \omega$	$0.51^{+0.20+0.15+0.68+0.40}_{-0.18-0.11-0.23-0.25}$	$0.15^{+0.05+0.07+0.02}_{-0.04-0.03-0.01}$	$0.90^{+0.08+0.10}_{-0.01-0.11}$	$1.3^{+0.1+0.1}_{-0.1-0.1}$
$\bar{B}_s^0 \to K^0 \phi$	$0.27^{+0.09+0.28+0.09+0.67}_{-0.08-0.14-0.06-0.18}$	$0.16^{+0.04+0.09+0.02}_{-0.03-0.04-0.01}$	$0.44^{+0.23+0.08}_{-0.18-0.07}$	$0.54^{+0.21+0.08}_{-0.17-0.07}$
$\bar{B}_s^0 \to \rho^0 \eta$	$0.17^{+0.03+0.07+0.02+0.02}_{-0.03-0.06-0.02-0.01}$	$0.06^{+0.03+0.01+0.00}_{-0.02-0.01-0.00}$	$0.08^{+0.04+0.01}_{-0.03-0.01}$	$0.06^{+0.03+0.00}_{-0.02-0.00}$
$\bar{B}_s^0 \to \rho^0 \eta'$	$0.25^{+0.06+0.10+0.02+0.02}_{-0.05-0.08-0.02-0.02}$	$0.13^{+0.06+0.02+0.00}_{-0.04-0.02-0.01}$	$0.003^{+0.082+0.000}_{-0.000-0.000}$	$0.14^{+0.24+0.01}_{-0.11-0.01}$
$\bar{B}_s^0 \to \omega \eta$	$0.012^{+0.005+0.010+0.028+0.025}_{-0.004-0.003-0.006-0.006}$	$0.04^{+0.03+0.05+0.00}_{-0.01-0.02-0.00}$	$0.04^{+0.04+0.00}_{-0.02-0.00}$	$0.007^{+0.011+0.001}_{-0.002-0.001}$
$\bar{B}_s^0 \to \omega \eta'$	$0.024^{+0.011+0.028+0.077+0.042}_{-0.009-0.006-0.010-0.015}$	$0.44^{+0.18+0.15+0.00}_{-0.13-0.14-0.01}$	$0.001^{+0.095+0.000}_{-0.000-0.000}$	$0.20^{+0.34+0.02}_{-0.17-0.02}$
$\bar{B}_s^0 \to \phi \eta$	$0.12^{+0.02+0.95+0.54+0.32}_{-0.02-0.14-0.12-0.13}$	$3.6^{+1.5+0.8+0.0}_{-1.0-0.6-0.0}$	$0.59^{+2.02+0.12}_{-0.59-0.10}$	$0.94^{+1.89+0.16}_{-0.97-0.13}$
$\bar{B}_s^0 \to \phi \eta'$	$0.05^{+0.01+1.10+0.18+0.40}_{-0.01-0.17-0.08-0.04}$	$0.19^{+0.06+0.19+0.00}_{-0.01-0.13-0.00}$	$7.3^{+7.7+1.6}_{-5.4-1.3}$	$4.3^{+5.2+0.7}_{-3.6-0.6}$
$\bar{B}_s^0 \to K^{*0} \eta$	$0.26^{+0.15+0.49+0.15+0.57}_{-0.13-0.22-0.05-0.15}$	$0.17^{+0.04+0.10+0.03}_{-0.04-0.06-0.01}$	$1.7^{+0.3+0.2}_{-0.3-0.1}$	$0.62^{+0.14+0.07}_{-0.14-0.08}$
$\bar{B}_s^0 \to K^{*0} \eta'$	$0.28^{+0.04+0.46+0.23+0.29}_{-0.04-0.24-0.10-0.15}$	$0.09^{+0.02+0.03+0.01}_{-0.02-0.02-0.01}$	$0.64^{+0.33+0.11}_{-0.26-0.11}$	$0.87^{+0.35+0.10}_{-0.32-0.08}$

ferent lifetimes of B^- and $\bar{B}^0$. The analysis is similar for the other two $b \to d$ modes: $B^- \to K^- K^{*0}$ and $\bar{B}^0 \to \bar{K}^0 K^{*0}$.

For the decays with sizable branching fractions, our predictions on direct *CP* asymmetries are typically small and most of them have the correct sign with experimental data. Predictions in QCDF approach on these channels are also small in magnitude, but some of them have different signs with our results and experimental data. In the PQCD approach, the strong phases mainly come from the $(S - P)(S + P)$ annihilation operators. These operators are chirally enhanced and the imaginary parts are dominant. Thus the direct *CP* asymmetries in the PQCD approach are typically large in magnitude.

C. $b \to s$ transitions without η and η'

Like $b \to d$ processes, $b \to s$ decay amplitudes can also be decomposed into three different parts according to the CKM matrix elements. The values of the CKM matrix elements are given by

$$\begin{aligned} |V_{ub} V_{us}^*| &= 0.81 \times 10^{-3}, \\ |V_{cb} V_{cs}^*| &= 39.41 \times 10^{-3}, \\ |V_{tb} V_{ts}^*| &= 40.66 \times 10^{-3}. \end{aligned} \tag{59}$$

Tree operators are highly CKM suppressed, but the CKM matrix elements for the other two kinds of contributions A_c and A_t are in similar size. Together with the hierarchy in Wilson coefficients, $C_{1,2} \gg C_{3-10}$, charming penguins will provide a dominant contribution. For example, the penguin operators in the $B^- \to \pi^- \bar{K}^0$ decay process is proportional to $a_4 + r_\chi a_6$, $B^- \to \pi^- \bar{K}^{*0}$ is proportional to a_4 while $B^- \to \rho^- \bar{K}^0$ is proportional to $a_4 - r_\chi a_6$, where $a_{4,6} = C_{4,6} + C_{3,5}/N_c$ and $r_\chi = 2\mu_P/m_b$. Thus if we only consider the emission diagrams, $\mathcal{BR}(B^- \to \pi^- \bar{K}^0) > \mathcal{BR}(B^- \to \pi^- \bar{K}^{*0}) > \mathcal{BR}(B^- \to \rho^- \bar{K}^0)$ holds, since $a_4 \sim a_6$ and $r_\chi \sim 1$. But in the present framework, contributions from penguin operators proportional to

TABLE VI. Direct CP asymmetries (in %) in the $B_s \to PV$ decays: the first solution (This work 1) and the second solution (This work 2). In both solutions, the chirally enhanced penguin has been taken into account in $B \to VP$ decay amplitudes. The first kind of uncertainties are from uncertainties in charming penguins and gluonic form factors which are discussed in the text; the second kinds of uncertainties are from those in the CKM matrix elements. We also cite theoretical results evaluated in QCDF [10] and PQCD [48] to make a comparison.

Modes	QCDF	PQCD	This work 1	This work 2
$\bar{B}_s^0 \to K^+ K^{*-}$	$2.2^{+0.6+8.4+5.1+68.6}_{-0.7-8.0-5.9-71.0}$	$-36.6^{+2.3+2.8+1.3}_{-2.3-3.5-1.2}$	$-11.2^{+19.1+1.3}_{-16.2-1.3}$	$-12.3^{+11.4+0.8}_{-11.3-0.8}$
$\bar{B}_s^0 \to K^{*+} K^-$	$-3.1^{+1.0+3.8+1.6+47.5}_{-1.1-2.6-1.3-45.0}$	$55.3^{+4.4+8.5+5.1}_{-4.9-9.8-2.5}$	$7.1^{+11.2+0.7}_{-12.4-0.7}$	$9.6^{+13.0+0.7}_{-13.5-0.9}$
$\bar{B}_s^0 \to K^0 \bar{K}^{*0}$	$1.7^{+0.4+0.6+0.5+1.4}_{-0.5-0.5-0.4-0.8}$	0	0	0
$\bar{B}_s^0 \to K^{*0} \bar{K}^0$	$0.2^{+0.0+0.2+0.1+0.2}_{-0.1-0.3-0.1-0.1}$	0	0	0
$\bar{B}_s^0 \to \pi^0 \phi$	$27.2^{+6.1+9.8+2.7+32.0}_{-6.8-5.6-2.4-37.1}$	$13.3^{+0.3+2.1+1.5}_{-0.4-1.7-0.7}$	0	0
$\bar{B}_s^0 \to \rho^0 \eta$	$27.8^{+6.4+9.1+2.6+25.9}_{-6.7-5.7-2.2-28.4}$	$-9.2^{+1.0+2.8+0.4}_{-0.4-2.7-0.7}$	0	0
$\bar{B}_s^0 \to \rho^0 \eta'$	$28.9^{+6.1+10.3+1.5+24.8}_{-7.5-6.3-1.8-27.5}$	$25.8^{+1.3+2.8+3.4}_{-2.0-3.6-1.5}$	0	0
$\bar{B}_s^0 \to \omega \eta$	$\cdots$	$-16.7^{+5.8+15.4+0.8}_{-3.2-19.1-1.7}$	0	0
$\bar{B}_s^0 \to \omega \eta'$	$\cdots$	$7.7^{+0.4+4.5+9.4}_{-0.1-4.2-0.4}$	0	0
$\bar{B}_s^0 \to \phi \eta$	$-8.4^{+2.0+30.1+14.6+36.3}_{-2.1-71.2-44.7-59.7}$	$-1.8^{+0.0+0.6+0.1}_{-0.1-0.6-0.2}$	$21.3^{+53.5+2.5}_{-83.2-2.6}$	$16.9^{+13.8+1.6}_{-18.3-1.6}$
$\bar{B}_s^0 \to \phi \eta'$	$-62.2^{+15.9+132.3+80.8+122.4}_{-10.2-84.2-46.8-49.9}$	$7.8^{+1.5+1.2+0.1}_{-0.5-8.6-0.4}$	$4.4^{+5.3+0.6}_{-7.1-0.6}$	$7.8^{+5.0+0.8}_{-4.9-0.8}$
$\bar{B}_s^0 \to \pi^- K^{*+}$	$0.6^{+0.2+1.4+0.1+19.9}_{-0.1-1.7-0.1-20.1}$	$-19.0^{+2.5+2.7+0.9}_{-2.6-3.4-1.4}$	$-9.9^{+17.2+0.9}_{-16.7-0.7}$	$-12.4^{+17.5+1.1}_{-15.3-1.2}$
$\bar{B}_s^0 \to \pi^0 K^{*0}$	$-45.7^{+14.3+13.0+28.4+80.0}_{-16.0-11.6-28.0-59.7}$	$-47.1^{+7.4+35.5+2.9}_{-8.7-29.8-7.0}$	$22.9^{+33.1+2.1}_{-40.2-1.9}$	$13.4^{+18.6+0.8}_{-18.8-1.2}$
$\bar{B}_s^0 \to \rho^- K^+$	$-1.5^{+0.4+1.2+0.2+12.1}_{-0.4-1.4-0.3-12.1}$	$14.2^{+2.4+2.3+1.2}_{-2.2-1.6-0.7}$	$11.8^{+17.5+1.2}_{-20.0-1.1}$	$10.8^{+9.4+0.9}_{-10.2-1.0}$
$\bar{B}_s^0 \to \rho^0 K^0$	$24.7^{+7.1+14.0+22.8+51.3}_{-5.2-12.4-17.7-52.3}$	$73.4^{+6.4+16.2+2.2}_{-11.7-47.8-3.9}$	$-12.0^{+20.1+1.0}_{-19.6-0.7}$	$-32.5^{+30.7+2.7}_{-23.4-2.9}$
$\bar{B}_s^0 \to K^0 \omega$	$-43.9^{+13.6+18.0+30.6+57.7}_{-13.4-18.2-30.2-49.3}$	$-52.1^{+3.2+22.7+3.2}_{-0.0-15.1-2.0}$	$24.4^{+33.7+2.2}_{-41.4-2.0}$	$18.2^{+16.4+1.2}_{-17.0-1.7}$
$\bar{B}_s^0 \to K^0 \phi$	$-10.3^{+3.0+4.7+3.7+5.0}_{-2.4-3.0-4.1-7.5}$	0	$-3.0^{+5.3+0.3}_{-4.7-0.3}$	$-2.2^{+3.0+0.1}_{-2.9-0.1}$
$\bar{B}_s^0 \to K^{*0} \eta$	$40.2^{+17.0+24.6+7.8+65.9}_{-11.5-30.8-14.0-96.3}$	$51.2^{+6.2+14.1+2.0}_{-6.4-12.4-3.3}$	$-25.7^{+23.4+2.0}_{-22.0-1.3}$	$-62.7^{+28.1+2.6}_{-22.5-3.9}$
$\bar{B}_s^0 \to K^{*0} \eta'$	$-58.6^{+16.9+41.4+19.9+44.9}_{-11.9-11.7-13.9-35.7}$	$-51.1^{+4.6+15.0+3.2}_{-6.6-18.2-4.1}$	$-35.2^{+63.3+3.1}_{-49.4-3.8}$	$-32.1^{+22.8+2.6}_{-23.2-1.7}$

$V_{tb}V_{ts}^*$ do not play the most important role:

$$\begin{aligned} |A_t(B^- \to \pi^- \bar{K}^0)| &= |0.16 \times (-0.044\zeta^P - 0.036\zeta_J^P)| \\ &\sim 15 \times 10^{-4}, \\ |A_t(B^- \to \rho^- \bar{K}^0)| &= |0.16 \times (0.0004\zeta^V + 0.004\zeta_J^V)| \\ &\sim 1 \times 10^{-4}, \\ |A_t(B^- \to \pi^- \bar{K}^{*0})| &= |0.217 \times (-0.022\zeta^P - 0.015\zeta_J^P)| \\ &\sim 10 \times 10^{-4}. \end{aligned} \tag{60}$$

Compared with the results given in Eqs. (50) and (54), we find penguin operators are smaller than charming penguins. According to the size of charming penguins, we expect the relation $\mathcal{BR}(B^- \to \rho^- \bar{K}^0) \sim \mathcal{BR}(B^- \to \pi^- \bar{K}^{*0})$. This is consistent with the experimental data.

From Table IV, we can see the direct CP asymmetries of $B^- \to \bar{K}^{*0}\pi^-$, $B^- \to \bar{K}^0\rho^-$, $B^- \to K^-\phi$, and $B^- \to \bar{K}^0\phi$ are zero. In these channels, tree operators do not contribute. The weak phases for penguin operators and charming penguins are equal to each other, which cannot induce any direct CP violations. CP asymmetries in other channels are not large, because the strong phases of charming penguins are either close to 0° or 180° and imaginary parts are accordingly small. The PQCD results for most $B \to K^*\pi$ and $B \to \rho K$ channels are much larger than ours, since they have more large imaginary parts from annihilation diagrams. The QCDF results are small and comparable with ours but with a relative minus sign. We have to wait for the experiment data to resolve this disagreements.

D. B Decays involving η or η'

As we can see from Table I, there is about 3.1σ deviation for our prediction on the branching ratio of $B^- \to \rho^-\eta'$ from the experimental data. Contributions from penguin operators are suppressed by the Wilson coefficients and the dominant contribution is from the tree operator. This kind of contribution is either proportional to the $B \to \eta_q$ or $B \to \eta_s$ form factor. Utilizing results given in Eqs. (50) and (54), we obtain $B \to \eta_q$ and $B \to \eta_s$ form factors as follows:

$$\begin{aligned} F^{B\to\eta_q} &= (\zeta^P + \zeta_J^P + 2\zeta_g + 2\zeta_{Jg}) \\ &= (0.053 \pm 0.068)[(0.100 \pm 0.021)], \\ F^{B\to\eta_s} &= (\zeta_g + \zeta_{Jg}) \\ &= (-0.076 \pm 0.055)[(-0.049 \pm 0.011)], \end{aligned} \tag{61}$$

where the results inside (outside) the square brackets are predictions using the second (first) kind of inputs. In Eq. (61), we can see that after taking the gluonic form

factors into account, the $F^{B\to\eta_q}$ and $F^{B\to\eta_s}$ form factors are a similar size but with different signs in both kinds of inputs. In $B^- \to \rho^- \eta_q$, another tree operator contributes in which η_q is emitted. Although this contribution is color suppressed, terms proportional to ζ_J^V give a sizable contribution. It can be estimated by using a larger effective $B \to \eta_q$ form factor. Recalling that physical states η and η' are mixtures of η_q and η_s as in Eq. (22), one obtains the expressions for $B \to \eta^{(\prime)}$ form factors:

$$\begin{aligned} F^{B\to\eta} &= \frac{F^{B\to\eta_q}}{\sqrt{2}}\cos(\theta) - F^{B\to\eta_s}\sin(\theta), \\ F^{B\to\eta'} &= \frac{F^{B\to\eta_q}}{\sqrt{2}}\sin(\theta) + F^{B\to\eta_s}\cos(\theta). \end{aligned} \tag{62}$$

The mixing angle between η_q and η_s has been determined as $\theta = (39.3 \pm 1.0)^\circ$ [33–35] which is very close to 45°, thus we can obtain very small $B \to \eta'$ form factors and relatively large $B \to \eta$ form factors. Thus the branching fraction of $B^- \to \rho^- \eta'$ is relatively suppressed for this flavor structure. In QCDF and PQCD approaches, the form factors are different: $F^{B\to\eta_q} \gg F^{B\to\eta_s}$. Thus the predicted branching ratio of $B^- \to \rho^- \eta$ is comparable with $\mathcal{BR}(B^- \to \rho^- \eta')$ in these two approaches.

As in the $\bar{B}^0 \to \pi^0\rho^0$ process, our predictions on branching fractions of $\bar{B}^0 \to \rho^0\eta^{(\prime)}$ and $\bar{B}^0 \to \omega\eta^{(\prime)}$ are much larger than the results evaluated in the QCDF and PQCD approaches. These channels are the so-called color-suppressed decays, as the contributions from terms proportional to ζ and ζ_g are small due to the small Wilson coefficients. But in the present framework, the hard-spectating form factors ζ_J and ζ_{Jg} are comparable with ζ and ζ_g. Moreover, the Wilson coefficients for these form factors are large. Thus branching ratios of $\bar{B}^0 \to \rho^0\eta^{(\prime)}$ and $\bar{B}^0 \to \omega\eta^{(\prime)}$ are much larger.

Similar with $B \to K^*\pi$ and $B \to \rho K$ decays, $B \to K^*\eta(\eta')$ are also induced by $b \to s$ transitions in which charming penguins provide most important contributions. But compared with $B \to K^*\pi$ and $B \to \rho K$ decays, there is something new in these channels. In $B \to K^*\eta(\eta')$, there exist three kinds of charming penguins:

$$A_{cc}^{K^*\eta_q} = \frac{1}{\sqrt{2}}(A_{cc}^{VP} + 2A_{ccg}^{VP}), \qquad A_{cc}^{K^*\eta_s} = A_{ccg}^{VP} + A_{cc}^{PV}. \tag{63}$$

Substituting the values given in Eqs. (50) and (54), we obtain ratios of charming penguins:

$$\frac{|\frac{\cos(\theta)}{\sqrt{2}}(A_{cc}^{VP} + 2A_{ccg}^{VP}) - \sin(\theta)(A_{ccg}^{VP} + A_{cc}^{PV})|^2}{|\frac{\cos(\theta)}{\sqrt{2}}(A_{cc}^{VP} + 2A_{ccg}^{VP}) + \sin(\theta)(A_{ccg}^{VP} + A_{cc}^{PV})|^2} \sim 2.0.$$

The branching fraction of $\bar{B}^0 \to \bar{K}^{*0}\eta$ is about 4 times larger than that of $\bar{B}^0 \to \bar{K}^{*0}\eta'$ for both solutions. The main reason for the difference is that $A_{cc}^{K^*\eta_s}$ is very small due to the cancellations between A_{cc}^{PV} and A_{ccg}^{VP}; the penguin operators play the dominant role in the $B \to K^*\eta_s$ decay amplitudes. Our results for these channels have a better agreement with experiments than QCDF and PQCD.

E. $B_s \to VP$ decays

Since we have assumed the SU(3) symmetry for form factors and charming penguins, branching fractions and direct CP asymmetries of the B_s decays are related to the corresponding B decays:

$$\begin{aligned} \mathcal{BR}(\bar{B}_s^0 \to K^{*+}K^-) &= \mathcal{BR}(\bar{B}^0 \to \rho^+K^-), \\ \mathcal{BR}(\bar{B}_s^0 \to K^+K^{*-}) &= \mathcal{BR}(\bar{B}^0 \to \pi^+K^{*-}), \end{aligned} \tag{64}$$

$$\begin{aligned} A_{CP}(\bar{B}_s^0 \to K^{*+}K^-) &= A_{CP}(\bar{B}^0 \to \rho^+K^-), \\ A_{CP}(\bar{B}_s^0 \to K^+K^{*-}) &= A_{CP}(\bar{B}^0 \to \pi^+K^{*-}). \end{aligned} \tag{65}$$

These relations can also be applied to the following channels:

$$\begin{aligned} \mathcal{BR}(\bar{B}_s^0 \to K^{*+}\pi^-) &= \mathcal{BR}(\bar{B}^0 \to \rho^+\pi^-), \\ \mathcal{BR}(\bar{B}_s^0 \to K^+\rho^-) &= \mathcal{BR}(\bar{B}^0 \to \pi^+\rho^-), \end{aligned} \tag{66}$$

$$\begin{aligned} A_{CP}(\bar{B}_s^0 \to K^{*+}\pi^-) &= A_{CP}(\bar{B}^0 \to \rho^+\pi^-), \\ A_{CP}(\bar{B}_s^0 \to K^+\rho^-) &= A_{CP}(\bar{B}^0 \to \pi^+\rho^-). \end{aligned} \tag{67}$$

In tree-operator-dominated processes $\bar{B}_s^0 \to \rho^-K^+$, we obtain branching ratios which are much smaller than predictions in the other two approaches—because PQCD predicts $F^{B_s\to K} = 0.24^{+0.05+0.00}_{-0.04-0.01}$ and QCDF use an even larger form factor $F^{B_s\to K} = 0.31 \pm 0.05$. $\mathcal{BR}(\bar{B}_s^0 \to \pi^-K^{*+})$ is consistent with results in the QCDF and PQCD approaches as the $B \to K^*$ form factors are consistent. As in B decays, we also predict larger branching ratios for color-suppressed B_s decays than QCDF and PQCD which can be tested in future experiments.

Our predictions on $b \to s$ processes $\bar{B}_s^0 \to K^*K$ are consistent with the other two approaches. But there are huge differences in our predictions of $\mathcal{BR}(\bar{B}_s \to \phi\eta(\eta'))$ with those in QCDF and PQCD. In the PQCD approach, contributions from gluonic components of η and η' in $B \to \eta^{(\prime)}$ form factors are very small and can be neglected [60]. As shown in Ref. [48], decay amplitudes of $B_s \to \phi\eta_q$ are dynamically enhanced sizably, as the Wilson coefficients $a_3 - a_5$ strongly depend on the factorization scale. In $B_s \to \phi\eta_s$, dominant penguin operators are either proportional to $a_4 - 2r_\chi a_6$ or a_4. The former Wilson coefficient is very small as $a_4 \sim a_6$ and $2r_\chi \sim 1$. The total decay amplitudes of $B_s \to \phi\eta_q$ and $B_s \to \phi\eta_s$ are in similar size but with different signs. Thus the branching ratio of $B_s \to \phi\eta$ predicted in the PQCD approach is relatively large while the branching ratio of $B_s \to \phi\eta'$ is small due to cancellations between the two amplitudes [48]. In the SCET framework, charming penguins play the most im-

portant role: the charming penguin A_{cc}^{VP} almost cancels with A_{cc}^{PV}. Thus the dominant contributions to $B_s \to \phi\eta(\eta')$ are from the gluonic charming penguin and the penguin operators which are proportional to $V_{tb}V_{ts}^*$. Neglecting the latter term, we have

$$A_{cc}^{B_s\to\phi\eta} = \cos(\theta)\sqrt{2}A_{ccg}^{VP} - \sin(\theta)A_{ccg}^{VP} \sim (\sqrt{2}-1)A_{ccg}^{VP},$$
$$A_{cc}^{B_s\to\phi\eta'} = \sin(\theta)\sqrt{2}A_{ccg}^{VP} + \cos(\theta)(A_{ccg}^{VP}) \sim (\sqrt{2}+1)A_{ccg}^{VP}. \quad (68)$$

These two equations can explain the small branching fraction for $B_s \to \phi\eta$ together with the large one for $B_s \to \phi\eta'$. The QCD penguin contributions do not change the ratios too much, but sizable differences appear in the two solutions. The large differences in two kinds of predictions on direct CP asymmetries also confirm this feature.

In B_s decays, there are 7 decays in which the direct CP asymmetries are zero: $\bar{B}_s \to K^{*0}\bar{K}^0$, $\bar{B}_s \to \bar{K}^{*0}K^0$, $\bar{B}_s \to \pi^0\phi$, and $\bar{B}_s \to \rho^0(\omega)\eta(')$. As we know, in order to give a nonvanishing direct CP violation, at least two decay amplitudes with different weak phases and different strong phases are required. In the first two decays, contributions from tree operators vanish at leading order. The nonzero contribution is either proportional to the CKM matrix elements $V_{tb}V_{ts}^*$ or $V_{cb}V_{cs}^*$ and both of them are taken real in our calculation. Thus in these two channels, there is only one weak phase and direct CP asymmetry is 0 in the present framework. The latter 5 channels are induced by $b \to s$ transitions and one of the final state mesons is neither open nor hidden strange. There is no contribution from charming penguins in these modes. The direct CP asymmetries are zero for lack of necessary strong phases.

F. Mixing-induced CP asymmetries

In this subsection, we will discuss mixing-induced CP asymmetries which can be studied via time-dependent measurements of decay widths. The four decay amplitudes in $B^0/\bar{B}^0 \to f(\bar{f})$ decays are defined by

$$A_f = \langle f|\mathcal{H}_{\rm eff}|B^0\rangle, \qquad \bar{A}_f = \langle f|\mathcal{H}_{\rm eff}|\bar{B}^0\rangle,$$
$$A_{\bar{f}} = \langle \bar{f}|\mathcal{H}_{\rm eff}|B^0\rangle, \qquad \bar{A}_{\bar{f}} = \langle \bar{f}|\mathcal{H}_{\rm eff}|\bar{B}^0\rangle. \quad (69)$$

Considering the width differences of the two mass eigenstates B_H and B_L, the decay amplitudes squared at time t of the state that was a pure B^0 state at time $t = 0$ can be parameterized by

$$|A_f(t)|^2 \equiv |\langle f|B(t)\rangle|^2 = \frac{e^{-\Gamma t}}{2}(|A_f|^2 + |\bar{A}_f|^2)\Big[\cosh\Big(\frac{\Delta\Gamma t}{2}\Big) + H_f \sinh\Big(\frac{\Delta\Gamma t}{2}\Big) + C_f\cos(\Delta m t) - S_f \sin(\Delta m t)\Big], \quad (70)$$

where $\Delta m = m_H - m_L > 0$ and $\Delta\Gamma = \Gamma_H - \Gamma_L$ is the difference of decay widths for the heavier and lighter B^0 mass eigenstates. The time-dependent decay amplitudes squared of another channel $\bar{B}^0 \to f$ is obtained from the above expression by flipping the signs of the $\cos(\Delta m t)$ and $\sin(\Delta m t)$ terms. For decays to the CP-conjugate final state, one replaces f by $\bar{f}$.

Time-dependent decay amplitudes squared can be simplified in two kinds of cases. In the B^0-$\bar{B}^0$ system, the small width difference $\Delta\Gamma$ can be safely neglected. Thus the first two terms $\cosh(\frac{\Delta\Gamma t}{2})$ and $\sinh(\frac{\Delta\Gamma t}{2})$ in Eq. (70) can be reduced to 1 and 0 and the decay amplitudes squared become

$$|A_f(t)|^2 \equiv |\langle f|B(t)\rangle|^2 = \frac{e^{-\Gamma t}}{2}(|A_f|^2 + |\bar{A}_f|^2)[1 + C_f\cos(\Delta m t) - S_f\sin(\Delta m t)], \quad (71)$$

In the following, we use the phase convention $CP|B^0\rangle = |\bar{B}^0\rangle$ and define the following amplitudes ratios:

$$\lambda_f = \frac{q}{p}\frac{\bar{A}_f}{A_f}, \qquad \lambda_{\bar{f}} = \frac{q}{p}\frac{\bar{A}_{\bar{f}}}{A_{\bar{f}}}, \quad (72)$$

and q and p are the mixing parameters between B^0 and $\bar{B}^0$. The definitions for C_f and S_f are given by

$$C_f = \frac{1-|\lambda_f|^2}{1+|\lambda_f|^2} = \frac{|A_f|^2 - |\bar{A}_f|^2}{|A_f|^2 + |\bar{A}_f|^2}, \qquad S_f = 2\frac{{\rm Im}(\lambda_f)}{1+|\lambda_f|^2},$$
$$C_{\bar{f}} = \frac{1-|\lambda_{\bar{f}}|^2}{1+|\lambda_{\bar{f}}|^2} = \frac{|A_{\bar{f}}|^2 - |\bar{A}_{\bar{f}}|^2}{|A_{\bar{f}}|^2 + |\bar{A}_{\bar{f}}|^2}, \qquad S_{\bar{f}} = 2\frac{{\rm Im}(\lambda_{\bar{f}})}{1+|\lambda_{\bar{f}}|^2}. \quad (73)$$

The system of four decay modes defines five asymmetry parameters, C_f, S_f, $C_{\bar{f}}$, $S_{\bar{f}}$ together with the global charge asymmetry related to the overall normalization:

$$A_{CP} = \frac{|A_f|^2 + |\bar{A}_f|^2 - |A_{\bar{f}}|^2 - |\bar{A}_{\bar{f}}|^2}{|A_f|^2 + |\bar{A}_f|^2 + |A_{\bar{f}}|^2 + |\bar{A}_{\bar{f}}|^2}. \quad (74)$$

One can also use the parameters $C \equiv \frac{1}{2}(C_f + C_{\bar{f}})$, $S \equiv \frac{1}{2}(S_f + S_{\bar{f}})$, $\Delta C \equiv \frac{1}{2}(C_f - C_{\bar{f}})$, $\Delta S \equiv \frac{1}{2}(S_f - S_{\bar{f}})$. If there is no direct CP violation, only two independent decay amplitudes squared are left. Thus $A_{CP} = 0$, $C_f = -C_{\bar{f}}$, and $S_f = -S_{\bar{f}}$ which also implies $C = 0$ and $S = 0$. If we recall that the CP invariance conditions at the decay amplitudes level are $A_f = \bar{A}_{\bar{f}}$ and $A_{\bar{f}} = \bar{A}_f$, one can study the following two parameters:

$$A_{f\bar{f}} = \frac{|\bar{A}_{\bar{f}}|^2 - |A_f|^2}{|\bar{A}_{\bar{f}}|^2 + |A_f|^2}, \qquad A_{\bar{f}f} = \frac{|\bar{A}_f|^2 - |A_{\bar{f}}|^2}{|\bar{A}_f|^2 + |A_{\bar{f}}|^2}. \quad (75)$$

Sometimes, they are considered as more physically intuitive parameters since they characterize direct CP viola-

TABLE VII. Mixing-induced CP asymmetries in $B \to \pi^{\pm}\rho^{\mp}$ decay processes: the first solution (This work 1) and the second solution (This work 2). In both cases, the chirally enhanced penguin has been taken into account. The first kind of uncertainties are from uncertainties in charming penguins which are discussed in the text; the second kinds of uncertainties are from those in the CKM matrix elements. We also cite theoretical results evaluated in the QCDF approach [10] to make a comparison.

Parameter	Exp.	QCDF	This work 1	This work 2
A_{CP}	-0.13 ± 0.04	$0.00^{+0.00+0.01+0.00+0.10}_{-0.00-0.01-0.00-0.10}$	$-0.12^{+0.04+0.04}_{-0.05-0.03}$	$-0.21^{+0.03+0.02}_{-0.02-0.03}$
C	0.01 ± 0.07	$0.00^{+0.00+0.01+0.00+0.02}_{-0.00-0.01-0.00-0.02}$	$-0.01^{+0.13+0.00}_{-0.12-0.00}$	$0.01^{+0.09+0.00}_{-0.10-0.00}$
S	0.01 ± 0.09	$0.13^{+0.60+0.04+0.02+0.02}_{-0.65-0.03-0.01-0.01}$	$-0.11^{+0.07+0.08}_{-0.08-0.13}$	$-0.01^{+0.06+0.08}_{-0.07-0.14}$
ΔC	0.37 ± 0.08	$0.16^{+0.06+0.23+0.01+0.01}_{-0.07-0.26-0.02-0.02}$	$0.11^{+0.12+0.01}_{-0.13-0.01}$	$0.12^{+0.09+0.01}_{-0.10-0.01}$
ΔS	-0.04 ± 0.10	$-0.02^{+0.01+0.00+0.00+0.01}_{-0.00-0.01-0.00-0.01}$	$-0.47^{+0.08+0.05}_{-0.06-0.04}$	$0.43^{+0.05+0.03}_{-0.07-0.03}$

tions. In $B^0 \to \rho^{\pm}\pi^{\mp}$ decays (choosing $f = \rho^+\pi^-$ and $\bar{f} = \rho^-\pi^+$), we use $A^{+-}_{\rho\pi}$ which parameterizes the direct CP violation in decays in which the produced ρ meson does not contain the spectator quark, while $A^{-+}_{\rho\pi}$ parameterizes the direct CP violation in decays in which it does. Of course, these two parameters are not independent of the other sets of parameters given above, and can be written as

$$A^{+-}_{\rho\pi} = -\frac{A_{CP} + C_{f\bar{f}} + A_{CP}\Delta C_{f\bar{f}}}{1 + \Delta C_{f\bar{f}} + A_{CP}C_{f\bar{f}}},$$
$$A^{-+}_{\rho\pi} = -\frac{A_{CP} + C_{f\bar{f}} + A_{CP}\Delta C_{f\bar{f}}}{-1 + \Delta C_{f\bar{f}} + A_{CP}C_{f\bar{f}}}. \quad (76)$$

Predictions on these parameters are given in Table VII. Most of them are consistent with the data except ΔC and ΔS.

If the final state f is a CP eigenstate, there are only two different amplitudes since $|f\rangle = \pm|\bar{f}\rangle$ and the time-dependent decay amplitudes squared can also be simplified. Restricting the final state f to have definite CP-parity, the time-dependent decay width for the $B \to f$ decay is

$$\Gamma(B^0(t) \to f) = e^{-\Gamma t}\bar{\Gamma}(B \to f) \times \left[\cosh\left(\frac{\Delta\Gamma t}{2}\right) + H_f \sinh\left(\frac{\Delta\Gamma t}{2}\right) - \mathcal{A}^{\rm dir}_{CP}\cos(\Delta m t) - S_f \sin(\Delta m t)\right]. \quad (77)$$

The time-dependent decay width $\Gamma(\bar{B}(t) \to f)$ is obtained from the above expression by flipping the signs of the $\cos(\Delta m t)$ and $\sin(\Delta m t)$ terms. In the B_d system, the width differences are small which can be safely neglected, but in the B_s system, we expect a much larger decay width difference $(\Delta\Gamma/\Gamma)_{B_s}$. This is estimated within the standard model to have a value $(\Delta\Gamma/\Gamma)_{B_s} = -0.147 \pm 0.060$ [61], while experimentally $(\Delta\Gamma/\Gamma)_{B_s} = -0.33^{+0.09}_{-0.11}$ [39], so that both S_f and H_f can be extracted from the time-dependent decays of B_s mesons. The definition of the various quantities in the above equation are as follows:

$$S_f = \frac{2\,\mathrm{Im}[\lambda]}{1 + |\lambda|^2}, \qquad H_f = \frac{2\,\mathrm{Re}[\lambda]}{1 + |\lambda|^2}, \quad (78)$$

with

$$\lambda = \eta_f \frac{q}{p}\frac{A(\bar{B} \to f)}{A(B \to \bar{f})}, \quad (79)$$

where η_f is $+1(-1)$ for a CP-even (CP-odd) final state f. $q/p = e^{-2i\beta}$ for the B_d system while $q/p = e^{+2i\epsilon}$ for the B_s system where $\epsilon = \arg[-V_{cb}V_{ts}V^*_{cs}V^*_{tb}]$. With the convention $\arg[V_{cb}] = \arg[V_{cs}] = 0$, the parameter can be reduced to $\epsilon = \arg[-V_{ts}V^*_{tb}]$. For $b \to s$ transition-induced $\bar{B}^0$ decays, the ratios of decay amplitudes $\frac{A(\bar{B} \to f)}{A(B \to \bar{f})}$ are almost real and thus $S_f \sim \sin(2\beta)$. These channels provide a good way to measure $\sin(2\beta)$. Experimentalists often use the following parameters in $b \to s$ transitions:

$$-\eta_f S_f = -2\frac{\mathrm{Im}[\frac{q}{p}\frac{A(\bar{B}_s \to f)}{A(B_s \to \bar{f})}]}{1 + |\lambda|^2},$$
$$-\eta_f H_f = -2\frac{\mathrm{Re}[\frac{q}{p}\frac{A(\bar{B}_s \to f)}{A(B_s \to \bar{f})}]}{1 + |\lambda|^2}, \quad (80)$$

while the latter parameter is only defined for the $B^0_s - \bar{B}^0_s$ system. Although the K^{*0} meson is not a CP eigenstate, its daughter-mesons $K_S\pi^0$ behave as CP eigenstates. Thus we also give the predictions on mixing-induced CP asymmetries in the decays involving a K^{*0} meson and other related decays. Results for these parameters are collected in Tables VIII and IX, where predictions on decays with branching ratios smaller than 10^{-7} are omitted.

After studying the two simplified cases, we come to the time-dependent CP asymmetries in $\bar{B}^0_s \to K^{*+}K^-$, where the final state is not a CP eigenstate and the width difference of $B^0_s - \bar{B}^0_s$ cannot be neglected either. In the following, we choose $f = K^{*+}K^-$ and $\bar{f} = K^+K^{*-}$. One needs to consider two additional CP asymmetries:

$$H_f = 2\frac{\mathrm{Re}(\lambda_f)}{1 + |\lambda_f|^2}, \qquad H_{\bar{f}} = 2\frac{\mathrm{Re}(\lambda_{\bar{f}})}{1 + |\lambda_{\bar{f}}|^2}, \quad (81)$$

which can be redefined as $H = \frac{H_f + H_{\bar{f}}}{2}$ and $\Delta H = \frac{H_f - H_{\bar{f}}}{2}$. Our predictions for these parameters are given in Table X, but we have not considered the global charge asymmetries

TABLE VIII. Mixing-induced CP asymmetries S_f in $B \to VP$ decay processes: the first solution (This work 1) and the second solution (This work 2). In both cases, the chirally enhanced penguin has been taken into account. The first kind of uncertainties are from uncertainties in charming penguins and gluonic form factors which are discussed in the text; the second kind of uncertainties are from those in the CKM matrix elements. We also quote the experimental results to make a comparison.

Channel	Exp.	This work 1	This work 2
$\bar{B}^0 \to \rho^0 K_S$	$0.61^{+0.22}_{-0.24} \pm 0.09 \pm 0.08$	$0.85^{+0.04+0.01}_{-0.05-0.01}$	$0.56^{+0.02+0.01}_{-0.03-0.01}$
$\bar{B}^0 \to \omega K_S$	0.48 ± 0.24	$0.51^{+0.05+0.02}_{-0.06-0.02}$	$0.80^{+0.02+0.01}_{-0.02-0.01}$
$\bar{B}^0 \to \phi K_S$	0.39 ± 0.17	0.69	0.69
$\bar{B}^0 \to K^{*-}\pi^+ \to K_S\pi^-\pi^+$	...	$0.93^{+0.04+0.01}_{-0.07-0.02}$	$0.34^{+0.06+0.03}_{-0.07-0.03}$
$\bar{B}^0 \to K^{*0}\pi^0 \to K_S\pi^0\pi^0$	...	$0.52^{+0.04+0.02}_{-0.05-0.02}$	$0.79^{+0.02+0.01}_{-0.02-0.01}$
$\bar{B}^0 \to K^{*0}\eta \to K_S\pi^0\eta$	...	$0.75^{+0.01+0.01}_{-0.01-0.01}$	$0.64^{+0.01+0.00}_{-0.01-0.00}$
$\bar{B}^0 \to K^{*0}\eta' \to K_S\pi^0\eta'$	...	$0.76^{+0.07+0.01}_{-0.06-0.01}$	$0.66^{+0.04+0.00}_{-0.05-0.00}$
$S(\bar{B}^0 \to \pi^0\rho^0)$	0.12 ± 0.38	$-0.11^{+0.14+0.10}_{-0.14-0.15}$	$-0.19^{+0.14+0.10}_{-0.14-0.15}$
$S(\bar{B}^0 \to \pi^0\omega)$	...	$-0.87^{+0.44+0.02}_{-0.00-0.01}$	$0.72^{+0.36+0.07}_{-1.54-0.11}$
$\bar{B}^0 \to \rho^0\eta$	...	$0.86^{+0.15+0.03}_{-2.03-0.07}$	$0.29^{+0.36+0.09}_{-0.44-0.15}$
$\bar{B}^0 \to \rho^0\eta'$	...	$0.79^{+0.20+0.05}_{-1.73-0.09}$	$0.38^{+0.22+0.09}_{-1.24-0.14}$
$\bar{B}^0 \to \omega\eta$	...	$0.12^{+0.19+0.10}_{-0.20-0.17}$	$-0.16^{+0.14+0.10}_{-0.15-0.15}$
$\bar{B}^0 \to \omega\eta'$	...	$0.23^{+0.59+0.10}_{-1.10-0.10}$	$-0.27^{+0.17+0.09}_{-0.33-0.14}$

because of the presence of $\Delta\Gamma$. These predictions will be tested at the forthcoming LHCb experiments

G. Isospin asymmetries and U-spin asymmetries

Currently, there are many experimental methods to measure CKM angles: α, β, and γ. But in order to reduce the uncertainties, a good way is to use SU(3) symmetry, although this will induce the errors from SU(3) symmetry breaking effect. Here we will present some tests on this kind of symmetry breaking, although the flavor SU(3) symmetry for $B \to P$, $B \to V$ form factors and various charming penguins are used.

In the $B \to \pi\pi$ and $B \to \pi\rho$ system, one often uses the following ratios [10]:

$$
\begin{aligned}
R_1 &\equiv \frac{\Gamma(\bar{B}^0 \to \pi^+\rho^-)}{\Gamma(\bar{B}^0 \to \pi^+\pi^-)}, \\
R_2 &\equiv \frac{\Gamma(\bar{B}^0 \to \pi^+\rho^-) + \Gamma(\bar{B}^0 \to \pi^-\rho^+)}{2\Gamma(\bar{B}^0 \to \pi^+\pi^-)}, \\
R_3 &\equiv \frac{\Gamma(\bar{B}^0 \to \pi^+\rho^-)}{\Gamma(\bar{B}^0 \to \pi^-\rho^+)}, \\
R_4 &\equiv \frac{2\Gamma(B^- \to \pi^-\rho^0)}{\Gamma(\bar{B}^0 \to \pi^-\rho^+)} - 1, \\
R_5 &\equiv \frac{2\Gamma(B^- \to \pi^0\rho^-)}{\Gamma(\bar{B}^0 \to \pi^+\rho^-)} - 1,
\end{aligned}
\tag{82}
$$

where the partial decay widths are CP averaged. Our predictions are given in Table XI, where we have used the experimental results on branching ratios to evaluate the ratios and these values are collected as experimental results. The predictions in the QCDF approach are also collected in this table. In $\bar{B}^0 \to \pi^+\pi^-$ and $\bar{B}^0 \to \pi^+\rho^-$, tree operators dominate. If we only consider the tree operators, R_1 becomes ratios of decay constants: $R_1 = (f_\rho/f_\pi)^2 \sim 2$. Our predictions are smaller than 2 for both solutions. In the first solution, the ratio is much smaller which is mainly caused by charming penguin terms: A_{cc}^{PP} gives a constructive contribution to the decay width of $\bar{B}^0 \to \pi^+\pi^-$ while A_{cc}^{VP} gives a destructive contribution to $\Gamma(\bar{B}^0 \to \pi^+\rho^-)$. In the second solution, the deviation of R_1 from 2 is not too large as the phase of A_{cc}^{PP} is almost the same as A_{cc}^{VP}. R_4 and R_5 are larger than the predictions in the QCDF approach and the present experimental data. $B^- \to \pi^-\rho^0$ contains two different contributions from tree operators: color-allowed contribution with ρ^- emitted; color-suppressed contribution with π^- emitted. In QCDF approach, the second contribution is small and the first contribution is related to tree operators in $B^- \to \pi^-\rho^+$. Neglecting the color-suppressed contribution and contributions from penguin operators, R_4 is equal to zero. In SCET, color-suppressed tree operators can give sizable contributions as we have discussed. Thus the branching ratio of $B^- \to \pi^-\rho^0$ is enhanced which can give a large value for R_4. The analysis is also similar for the ratio R_5.

In $\bar{B}_d^0 \to K^{*-}\pi^+$, $\bar{B}_s^0 \to K^+\rho^-$, $\bar{B}_d^0 \to K^-\rho^+$, and $\bar{B}_s^0 \to K^{*+}\pi^-$, the branching ratios are very different from each other due to the differing strong and weak phases entering in the tree and penguin amplitudes. However, as shown by Gronau [62], the two relevant products of the CKM matrix elements entering in the expressions for the direct CP asymmetries in these decays are equal, and, as stressed by Lipkin [63] subsequently, the final states in these decays are charge conjugates, and the strong interactions being

TABLE IX. Mixing-induced CP asymmetries $(S_f)_{B_s}$ and $(H_f)_{B_s}$ in $B_s \to PV$ decays. Results obtained in the PQCD approach [48] are also collected here; the errors for these entries correspond to the uncertainties in the input hadronic quantities (charming penguins and the two form factors ζ_g and ζ_{Jg}), and the CKM matrix elements, respectively.

Modes	PQCD	This work 1	This work 2
$\bar{B}_s^0 \to \pi^0\phi$	$-0.07^{+0.01+0.08+0.02}_{-0.01-0.09-0.03}$	$0.89^{+0.00+0.04}_{-0.00-0.05}$	$0.90^{+0.00+0.02}_{-0.00-0.03}$
	$0.98^{+0.00+0.01+0.01}_{-0.00-0.03-0.00}$	$-0.45^{+0.00+0.09}_{-0.00-0.10}$	$0.44^{+0.00+0.05}_{-0.00-0.05}$
$\bar{B}_s^0 \to \rho^0\eta$	$0.15^{+0.06+0.14+0.01}_{-0.06-0.16-0.01}$	$1.00^{+0.00+0.00}_{-0.06-0.01}$	$0.60^{+0.30+0.03}_{-0.53-0.03}$
	$0.98^{+0.01+0.01+0.00}_{-0.01-0.03-0.00}$	$-0.04^{+0.41+0.08}_{-0.32-0.08}$	$0.80^{+0.20+0.02}_{-0.36-0.02}$
$\bar{B}_s^0 \to \rho^0\eta'$	$-0.16^{+0.00+0.10+0.04}_{-0.00-0.12-0.05}$	$0.95^{+0.00+0.02}_{-1.60-0.02}$	$-0.41^{+0.75+0.10}_{-0.75-0.15}$
	$0.95^{+0.01+0.01+0.01}_{-0.00-0.02-0.02}$	$0.32^{+0.67+0.06}_{-1.29-0.06}$	$-0.91^{+0.82+0.08}_{-0.08-0.04}$
$\bar{B}_s^0 \to \omega\eta$	$-0.02^{+0.01+0.02+0.00}_{-0.03-0.08-0.00}$	$-0.62^{+0.41+0.08}_{-0.18-0.12}$	$0.93^{+0.04+0.03}_{-0.98-0.04}$
	$0.99^{+0.01+0.01+0.00}_{-0.01-0.06-0.00}$	$-0.79^{+0.16+0.11}_{-0.20-0.06}$	$-0.37^{+1.37+0.09}_{-0.65-0.10}$
$\bar{B}_s^0 \to \omega\eta'$	$-0.11^{+0.01+0.04+0.02}_{-0.00-0.04-0.03}$	$-0.25^{+1.23+0.10}_{-0.74-0.16}$	$-1.00^{+0.04+0.01}_{-0.00-0.00}$
	$0.99^{+0.00+0.00+0.00}_{-0.00-0.00-0.00}$	$-0.97^{+2.12+0.05}_{-0.00-0.02}$	$-0.09^{+0.32+0.12}_{-0.22-0.08}$
$\bar{B}_s^0 \to \phi\eta$	$-0.03^{+0.02+0.07+0.01}_{-0.01-0.20-0.02}$	$-0.39^{+0.43+0.04}_{-0.15-0.04}$	$0.23^{+0.35+0.02}_{-0.16-0.02}$
	$1.00^{+0.00+0.00+0.00}_{-0.00-0.01-0.00}$	$0.90^{+0.14+0.02}_{-0.24-0.02}$	$0.96^{+0.04+0.01}_{-0.12-0.01}$
$\bar{B}_s^0 \to \phi\eta'$	$0.00^{+0.00+0.02+0.00}_{-0.00-0.02-0.00}$	$-0.07^{+0.06+0.01}_{-0.06-0.01}$	$0.10^{+0.07+0.01}_{-0.05-0.01}$
	$1.00^{+0.00+0.00+0.00}_{-0.00-0.00-0.02}$	$1.00^{+0.00+0.00}_{-0.01-0.00}$	$0.99^{+0.01+0.00}_{-0.01-0.00}$
$\bar{B}_s^0 \to K_S\phi$	-0.72	$0.09^{+0.04+0.01}_{-0.03-0.01}$	$-0.13^{+0.02+0.01}_{-0.02-0.01}$
	-0.69	$-1.00^{+0.00+0.00}_{-0.00-0.00}$	$-0.99^{+0.00+0.00}_{-0.00-0.00}$
$\bar{B}_s^0 \to \rho^0 K_S$	$-0.57^{+0.22+0.51+0.02}_{-0.17-0.39-0.05}$	$0.99^{+0.00+0.00}_{-0.05-0.01}$	$-0.03^{+0.22+0.17}_{-0.17-0.12}$
	$-0.36^{+0.10+0.46+0.04}_{-0.13-0.15-0.04}$	$0.04^{+0.13+0.09}_{-0.11-0.13}$	$0.95^{+0.05+0.01}_{-0.13-0.02}$
$\bar{B}_s^0 \to K_S\omega$	$-0.63^{+0.09+0.28+0.01}_{-0.09-0.11-0.02}$	$-0.11^{+0.28+0.18}_{-0.22-0.14}$	$0.98^{+0.02+0.00}_{-0.04-0.01}$
	$-0.57^{+0.11+0.31+0.02}_{-0.13-0.38-0.02}$	$0.96^{+0.02+0.01}_{-0.16-0.03}$	$-0.07^{+0.11+0.08}_{-0.09-0.12}$
$\bar{B}_s^0 \to K^{*+}\pi^- \to K_S\pi^+\pi^-$	$\ldots$	$0.98^{+0.01+0.01}_{-0.04-0.02}$	$0.35^{+0.11+0.15}_{-0.09-0.11}$
	$\ldots$	$0.16^{+0.11+0.09}_{-0.09-0.13}$	$0.93^{+0.03+0.03}_{-0.07-0.07}$
$\bar{B}_s^0 \to K^{*0}\pi^0 \to K_S\pi^0\pi^0$	$\ldots$	$-0.07^{+0.26+0.18}_{-0.22-0.14}$	$0.94^{+0.03+0.02}_{-0.05-0.04}$
	$\ldots$	$0.97^{+0.01+0.01}_{-0.15-0.02}$	$-0.30^{+0.12+0.07}_{-0.09-0.10}$
$\bar{B}_s^0 \to K^{*0}\eta \to K_S\pi^0\eta$	$\ldots$	$0.94^{+0.06+0.02}_{-0.09-0.03}$	$-0.77^{+0.23+0.04}_{-0.16-0.03}$
	$\ldots$	$-0.22^{+0.15+0.08}_{-0.14-0.11}$	$0.10^{+0.26+0.11}_{-0.22-0.11}$
$\bar{B}_s^0 \to K^{*0}\eta' \to K_S\pi^0\eta'$	$\ldots$	$-0.94^{+0.33+0.03}_{-0.09-0.01}$	$0.72^{+0.15+0.04}_{-0.16-0.05}$
	$\ldots$	$0.01^{+0.45+0.16}_{-0.39-0.16}$	$-0.62^{+0.20+0.05}_{-0.16-0.06}$

TABLE X. Mixing-induced CP asymmetries in $\bar{B}_s^0 \to K^{*+}K^-$ decay processes: the first solution (This work 1) and the second solution (This work 2). In both predictions, we have included the chirally enhanced penguin and chosen $f = K^{*+}K^-$. The first kind of uncertainties are from uncertainties in charming penguins which are discussed in the text; the second kind of uncertainties are from those in the CKM matrix elements.

Parameter	This work 1	This work 2
C	$0.02^{+0.10+0.00}_{-0.11-0.00}$	$0.01^{+0.09+0.00}_{-0.09-0.00}$
S	$-0.02^{+0.07+0.01}_{-0.07-0.01}$	$0.02^{+0.05+0.01}_{-0.05-0.00}$
H	$0.92^{+0.02+0.02}_{-0.04-0.02}$	$0.91^{+0.02+0.02}_{-0.03-0.02}$
ΔC	$-0.09^{+0.11+0.01}_{-0.10-0.01}$	$-0.11^{+0.09+0.01}_{-0.09-0.01}$
ΔS	$0.38^{+0.07+0.04}_{-0.07-0.04}$	$-0.41^{+0.05+0.03}_{-0.05-0.03}$
ΔH	$0.01^{+0.04+0.00}_{-0.02-0.00}$	$0.01^{+0.02+0.00}_{-0.02-0.00}$

TABLE XI. Two kinds of results for the ratios R_{1-5} in $B \to \pi\pi$ and $B \to \pi\rho$ decays, together with the predictions in QCDF [10] and experimental data evaluated using the results of branching fractions. The first kind of uncertainties are from uncertainties in charming penguins as discussed in the text; the second kind of uncertainties are from those in the CKM matrix elements.

	Exp.	QCDF	This work 1	This work 2
R_1	$2.69^{+0.54}_{-0.53}$	$2.39^{+0.31+0.04+0.15+0.05}_{-0.25-0.08-0.12-0.11}$	$1.32^{+0.15+0.10}_{-0.12-0.12}$	$1.84^{+0.22+0.05}_{-0.19-0.06}$
R_2	$2.21^{+0.37}_{-0.37}$	$2.06^{+0.40+0.53+0.12+0.03}_{-0.30-0.36-0.09-0.06}$	$1.17^{+0.13+0.06}_{-0.11-0.07}$	$1.52^{+0.17+0.07}_{-0.15-0.09}$
R_3	$1.56^{+0.68}_{-0.46}$	$1.38^{+0.18+0.82+0.03+0.02}_{-0.17-0.59-0.04-0.05}$	$1.28^{+0.12+0.08}_{-0.10-0.10}$	$1.54^{+0.07+0.11}_{-0.09-0.07}$
R_4	$0.96^{+0.80}_{-0.49}$	$0.42^{+0.04+0.15+0.45+0.23}_{-0.04-0.11-0.21-0.20}$	$2.38^{+0.21+0.02}_{-0.20-0.02}$	$1.23^{+0.04+0.02}_{-0.04-0.02}$
R_5	$0.57^{+0.43}_{-0.33}$	$0.22^{+0.07+0.08+0.23+0.14}_{-0.08-0.06-0.12-0.12}$	$1.21^{+0.05+0.02}_{-0.05-0.03}$	$1.09^{+0.08+0.04}_{-0.08-0.03}$

charge-conjugation invariant, the direct CP asymmetry in $\bar{B}_s^0 \to K^+\pi^-$ can be related to the well-measured CP asymmetry in the decay $\bar{B}_d^0 \to K^-\pi^+$ using U-spin symmetry. In this symmetry limit, we have [62,63]

$$|A(B_s^0 \to \pi^+ K^{*-})|^2 - |A(\bar{B}_s^0 \to \pi^- K^{*+})|^2 = |A(\bar{B}_d \to \rho^+ K^-)|^2 - |A(B_d \to \rho^- K^+)|^2, \quad (83)$$

$$A_{CP}^{\rm dir}(\bar{B}_d \to \rho^+ K^-) = -A_{CP}^{\rm dir}(\bar{B}_s^0 \to \pi^- K^{*+}) \cdot \frac{\mathrm{BR}(\bar{B}_s^0 \to \pi^- K^{*+})}{\mathrm{BR}(\bar{B}_d^0 \to \rho^+ K^-)} \cdot \frac{\tau(B_d)}{\tau(B_s)}. \quad (84)$$

Following the suggestions in the literature, we can test these equations and search for possible new physics effects which would likely violate these relations. Accordingly, one can define the following parameters:

$$R_6 \equiv \frac{|A(B_s \to \pi^+ K^{*-})|^2 - |A(\bar{B}_s \to \pi^- K^{*+})|^2}{|A(B_d \to \rho^- K^+)|^2 - |A(\bar{B}_d \to \rho^+ K^-)|^2} = \frac{\mathcal{BR}(\bar{B}_s \to \pi^- K^{*+}) A_{CP}^{\rm dir}(\bar{B}_s \to \pi^- K^{*+}) \tau(B_d)}{\mathcal{BR}(\bar{B} \to K^- \rho^+) A_{CP}^{\rm dir}(\bar{B} \to K^- \rho^+) \tau(B_s)}, \quad (85)$$

$$\Delta_1 = \frac{A_{CP}^{\rm dir}(\bar{B}_d \to \rho^+ K^-)}{A_{CP}^{\rm dir}(\bar{B}_s \to \pi^- K^{*+})} + \frac{\mathrm{BR}(B_s \to \pi^+ K^{*-})}{\mathrm{BR}(\bar{B}_d \to \rho^+ K^-)} \cdot \frac{\tau(B_d)}{\tau(B_s)}, \quad (86)$$

$$R_7 \equiv \frac{|A(B_s \to \rho^+ K^-)|^2 - |A(\bar{B}_s \to \rho^- K^+)|^2}{|A(B_d \to \rho^- K^+)|^2 - |A(\bar{B}_d \to \rho^+ K^-)|^2} = \frac{\mathcal{BR}(\bar{B}_s \to \rho^- K^+) A_{CP}^{\rm dir}(\bar{B}_s \to \rho^- K^+) \tau(B_d)}{\mathcal{BR}(\bar{B} \to K^{*-} \pi^+) A_{CP}^{\rm dir}(\bar{B} \to K^{*-} \rho^+) \tau(B_s)}, \quad (87)$$

$$\Delta_2 = \frac{A_{CP}^{\rm dir}(\bar{B}_d \to \pi^+ K^{*-})}{A_{CP}^{\rm dir}(\bar{B}_s \to \rho^- K^+)} + \frac{\mathrm{BR}(\bar{B}_s \to \rho^- K^+)}{\mathrm{BR}(\bar{B}_d \to \pi^+ K^{*-})} \cdot \frac{\tau(B_d)}{\tau(B_s)}. \quad (88)$$

We also consider $\bar{B}^0 \to \pi^+\rho^-$, $\bar{B}_s^0 \to K^+ K^{*-}$, $\bar{B}^0 \to \pi^-\rho^+$, and $\bar{B}_s^0 \to K^{*+} K^-$ which are related by U-spin transformation and define the following ratios:

$$R_8 \equiv \frac{|A(B_s \to K^{*+} K^-)|^2 - |A(\bar{B}_s \to K^{*-} K^+)|^2}{|A(B_d \to \rho^+ \pi^-)|^2 - |A(\bar{B}_d \to \rho^- \pi^+)|^2} = \frac{\mathcal{BR}(\bar{B}_s \to K^+ K^{*-}) A_{CP}^{\rm dir}(\bar{B}_s \to K^+ K^{*-}) \tau(B_d)}{\mathcal{BR}(\bar{B} \to \pi^+ \rho^-) A_{CP}^{\rm dir}(\bar{B} \to \pi^+ \rho^-) \tau(B_s)}, \quad (89)$$

$$\Delta_3 = \frac{A_{CP}^{\rm dir}(\bar{B}_d \to \rho^- \pi^+)}{A_{CP}^{\rm dir}(\bar{B}_s \to K^{*-} K^+)} + \frac{\mathrm{BR}(\bar{B}_s \to K^{*-} K^+)}{\mathrm{BR}(\bar{B}_d \to \rho^- \pi^+)} \cdot \frac{\tau(B_d)}{\tau(B_s)}, \quad (90)$$

$$R_9 \equiv \frac{|A(B_s \to K^+ K^{*-})|^2 - |A(\bar{B}_s \to K^- K^{*+})|^2}{|A(B_d \to \pi^+ \rho^-)|^2 - |A(\bar{B}_d \to \pi^- \rho^+)|^2} = \frac{\mathcal{BR}(\bar{B}_s \to K^- K^{*+}) A_{CP}^{\rm dir}(\bar{B}_s \to K^- K^{*+}) \tau(B_d)}{\mathcal{BR}(\bar{B} \to \pi^- \rho^+) A_{CP}^{\rm dir}(\bar{B} \to \pi^- \rho^+) \tau(B_s)}, \quad (91)$$

$$\Delta_4 = \frac{A_{CP}^{\rm dir}(\bar{B}_d \to \pi^- \rho^+)}{A_{CP}^{\rm dir}(\bar{B}_s \to K^- K^{*+})} + \frac{\mathrm{BR}(\bar{B}_s \to K^- K^{*+})}{\mathrm{BR}(\bar{B}_d \to \pi^- \rho^+)} \cdot \frac{\tau(B_d)}{\tau(B_s)}. \quad (92)$$

In the flavor SU(3) symmetry limit, the ratios are $R = -1$ and Δ is zero. Using the first solution for the 16 inputs, we obtain the following values:

$$\begin{aligned} R_6 &= -0.89, & \Delta_1 &= -0.08^{+0.02+0.01}_{-0.04-0.01}, \\ R_7 &= -0.99, & \Delta_2 &= -0.01^{+0.00+0.00}_{-0.01-0.00}, \\ R_8 &= -1.11, & \Delta_3 &= 0.11^{+0.06+0.03}_{-0.05-0.02}, \\ R_9 &= -1.24, & \Delta_4 &= 0.33^{+0.12+0.06}_{-0.11-0.05}, \end{aligned} \tag{93}$$

where the tiny uncertainties of R_{6-8} are omitted here. Our predictions using the second kind of inputs are given by

$$\begin{aligned} R_6 &= -0.87, & \Delta_1 &= -0.10^{+0.03+0.02}_{-0.05-0.02}, \\ R_7 &= -0.99, & \Delta_2 &= -0.01^{+0.00+0.00}_{-0.00-0.00}, \\ R_8 &= -1.10, & \Delta_3 &= 0.09^{+0.03+0.01}_{-0.02-0.01}, \\ R_9 &= -1.25, & \Delta_4 &= 0.33^{+0.13+0.06}_{-0.11-0.05}. \end{aligned} \tag{94}$$

Since the form factors and charming penguins are assumed to the respective flavor SU(3) symmetry, the small deviations for the ratios R and Δ are reasonable.

V. COMPARISONS WITH THE PQCD APPROACH

The PQCD approach is based on k_T factorization, where one keeps the intrinsic transverse momentum of quark degrees of freedom. The intrinsic transverse momentum can smear the end-point singularities which often appear in collinear factorization. Resummation of double logarithms results in the Sudakov factor which suppresses contributions from the end-point region to make the PQCD approach more self-consistent. This approach can explain many problems to achieve great successes. Currently, radiative corrections [46,64–66] and power corrections in $1/m_b$ [67,68] in this approach are under studies. In the PQCD approach, annihilation diagrams can be directly calculated. Among them, the $(S-P)(S+P)$ annihilation penguin operators [from the Fierz transformation of $(V-A)(V+A)$ operators] are the most important ones. According to the power counting in the PQCD approach, annihilation diagrams are suppressed by $\Lambda_{\rm QCD}/m_b$ but the suppression for $(S-P)(S+P)$ annihilation penguin operators is $2r_\chi$. This factor is comparable with 1. Thus annihilations play a very important role in the PQCD approach. Phenomenologically, the large annihilations can explain the correct branching ratios and direct CP asymmetries of $B^0 \to \pi^+\pi^-$ and $\bar{B}^0 \to K^-\pi^+$ [69], the polarization problem of $B \to \phi K^*$ [70], etc. In Fig. 2(a), we draw the Feynman diagrams for this term. Comparing with charming penguins, we can see they have the same topologies in flavor space. So generally speaking, charming penguins in SCET as shown in Fig. 2(b) have the same role with $(S-P)(S+P)$ annihilation penguin operators in PQCD. Both of them are essential to explaining the branching ratios in these two different approaches. But there are indeed some differences in predictions on other parameters

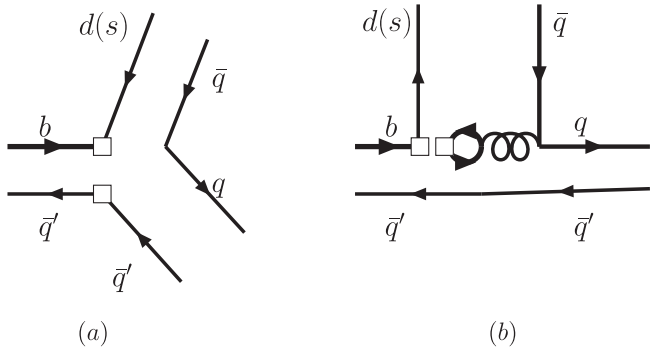

FIG. 2. Feynman diagrams for the $(S-P)(S+P)$ annihilation operators in the PQCD approach and charming penguins in SCET.

such as direct CP asymmetries and mixing-induced CP asymmetries.

First of all, the CKM matrix elements associated with charming penguins and $(S-P)(S+P)$ annihilation penguin operators are different. If we consider $\bar{B}$ decays in which a b quark annihilates, the $(S-P)(S+P)$ annihilation penguin operators are proportional to $V_{tb}V_{tD}^*$, while charming penguins are proportional to $V_{cb}V_{cD}^*$. The differences in the CKM matrix elements will affect direct CP asymmetries and mixing-induced CP asymmetries sizably. For example, in $\bar{B}_s^0 \to \phi K_S$ decay, the mixing-induced CP asymmetries in SCET are dramatically different from predictions in the PQCD approach. In the SCET framework, there are no contributions from tree operators to $B_s \to \phi K_S$ at tree level and penguin operators are much smaller than charming penguins. As the CKM matrix element $V_{cb}V_{cD}^*$ for the charming penguin is real, the parameter λ defined in Eq. (79) becomes $\lambda = -e^{+2i\epsilon}$, where we have neglected contributions from penguin operators. Thus in SCET the two parameters S_f and H_f are given by

$$\begin{aligned} S_f &= -\sin(2\epsilon) = -0.03, \\ H_f &= -\cos(2\epsilon) = -1.00. \end{aligned} \tag{95}$$

In the PQCD approach, the CKM matrix element for the $(S-P)(S+P)$ annihilation penguin operators is $V_{tb}V_{td}^*$ which gives $\lambda = -e^{+2i\epsilon+2i\beta}$:

$$\begin{aligned} S_f &= -\sin(2\epsilon+2\beta) = -0.72, \\ H_f &= -\cos(2\epsilon+2\beta) = -0.69. \end{aligned} \tag{96}$$

The differences in the mixing-induced CP asymmetries between SCET and PQCD will be tested in future experiments.

In the PQCD approach, contributions from the $(S-P)(S+P)$ annihilation penguin operators can be calculated using perturbation theory. These contributions are expressed as the convolution of light-cone distribution amplitudes and a hard kernel. We can also include SU(3) symmetry breaking effects in the calculation in PQCD approach. In SCET, charming penguins are from the charm

quark loops. Since the charm quark is heavy, one cannot factorize charming penguins (see Refs. [8–10,71] for another point of view). Thus charming penguins are nonperturbative in nature which is similar with the final state interactions [72,73]. In the present work based on SCET, we have assumed SU(3) symmetries for the contributions from charming penguins. The magnitudes and strong phases of charming penguins cannot be calculated using perturbation theory which was obtained by fitting the experimental data.

The third difference is the magnitudes of charming penguins in SCET and contributions from the $(S-P)\times(S+P)$ annihilation penguin operators in the PQCD approach. This difference arises from the different power counting in the two approaches. We take $b\to s$ transitions to illustrate the difference. In the PQCD approach, the $(S-P)(S+P)$ annihilation penguins are enhanced to be of the same order with penguins in emission diagrams. In SCET, charming penguins are more important. Comparing the values given in Eqs. (50), (54), and (60), we can see charming penguins in SCET always larger than contributions from emission penguin diagrams.

In the PQCD approach, the $(S-P)(S+P)$ annihilation penguin operators are chirally enhanced and the dominant contribution is from the imaginary part. The main strong phases in the PQCD approach which are essential to explaining the large CP asymmetries in many channels are also produced through these operators. But in SCET, as we have shown in Eqs. (50) and (54), strong phases of charming penguins are not too large. Accordingly, our predictions on direct CP asymmetries are small compared with predictions in the PQCD approach.

VI. CONCLUSIONS

We provide the analysis of charmless two-body $B\to VP$ decays under the framework of soft collinear effective theory. Besides the leading power contributions, we also take some power corrections (chirally enhanced penguins) into account. In the present framework, decay amplitudes of $B\to PP$ and $B\to VP$ decay channels can be expressed as functions of 16 nonperturbative inputs: 6 form factors and 5 complex (10 real) charming penguins. Using the $B\to PP$ and $B\to VP$ experimental data on branching fractions and CP asymmetry variables, we find two kinds of solutions in χ^2 fit for these 16 nonperturbative inputs. A chirally enhanced penguin could change some charming penguins sizably, since they have the same topology with each other. However, most other nonperturbative inputs and predictions on branching ratios and CP asymmetries are not changed too much. With the two sets of inputs, we predict branching fractions and CP asymmetries. Agreements and differences with results in QCD factorization and perturbative QCD approach are also analyzed. Our conclusions are as follows:

(i) In color-allowed processes such as $\bar{B}^0\to\pi^\pm\rho^\mp$ decays, tree operators provide the dominant contributions. Our predictions on branching fractions are smaller than the ones calculated in the QCDF approach and PQCD approach. The main reason is that both $B\to P$ and $B\to V$ form factors in SCET are smaller. $B^0\to\pi^0\rho^0$ and other color-suppressed channels are predicted with larger branching ratios in SCET, because the hard-scattering form factors $\zeta_J^{P,V}$ are comparable with $\zeta^{P,V}$ which also have large Wilson coefficients. The large branching ratios for $B^0\to\pi^0\rho^0$ are consistent with the experimental data.

(ii) $b\to s$ decay processes such as $B\to\pi K^*$, $B\to\rho K$ and the corresponding B_s decays are dominated by contributions from charming penguins. Since we have assumed flavor SU(3) symmetry for charming penguins, branching fractions of $b\to s$ transition decays can be estimated by analyzing the corresponding charming penguin terms. Decays with isosinglet mesons η and η' are slightly different since there exists cancellations between different charming penguins.

(iii) In the PQCD approach, annihilation diagrams do not suffer from the end-point singularity problem, which can be directly calculated. Among the three kinds of penguin operators, the $(S-P)(S+P)$ operators are most important which provide the main strong phase in the PQCD approach. In the SCET framework, charming penguins play an important role especially in $b\to s$ transitions. The $(S-P)(S+P)$ annihilations have the same topology as a charming penguin. Besides the commonalities, there exist many differences in these two objects including weak phases, magnitudes, strong phases, SU(3) symmetry property, and factorization property. These differences will mainly affect the direct CP asymmetries and time-dependent CP asymmetry variables.

ACKNOWLEDGMENTS

This work is partly supported by National Nature Science Foundation of China under Grants No. 10735080, No. 10625525, and No. 10705050. We would like to thank H.-Y. Cheng, T. Huang, Y. Jia, M. Z. Yang, Y. D. Yang, and Q. Zhao for valuable discussions and comments. W. Wang would like to acknowledge G. F. Cao and G. Li for the great help on the χ^2-fit program.

APPENDIX: EXPRESSIONS FOR HARD KERNELS

For explicit decay channels, the hard kernels depend on the Lorentz structure and flavor structures. They can be evaluated using the Wilson coefficients given in Eqs. (16) and (17). In this appendix, we intend to write the decay

amplitudes in a compact form. In doing so, the following meson matrices are required:

$$B^- = (1,0,0), \qquad \bar{B}^0 = (0,1,0), \qquad \bar{B}_s^0 = (0,0,1),$$

$$M_{\pi^+} = M_{\rho^+} = \begin{pmatrix} 0 & 0 & 0 \\ 1 & 0 & 0 \\ 0 & 0 & 0 \end{pmatrix},$$

$$M_{K^+} = M_{K^{*+}} = \begin{pmatrix} 0 & 0 & 0 \\ 0 & 0 & 0 \\ 1 & 0 & 0 \end{pmatrix},$$

$$M_{K^0} = M_{K^{*0}} = \begin{pmatrix} 0 & 0 & 0 \\ 0 & 0 & 0 \\ 0 & 1 & 0 \end{pmatrix},$$

$$\sqrt{2}M_{\pi^0} = \sqrt{2}M_{\rho^0} = \begin{pmatrix} 1 & 0 & 0 \\ 0 & -1 & 0 \\ 0 & 0 & 0 \end{pmatrix},$$

$$\sqrt{2}M_{\eta_q} = \sqrt{2}M_{\omega} = \begin{pmatrix} 1 & 0 & 0 \\ 0 & 1 & 0 \\ 0 & 0 & 0 \end{pmatrix},$$

$$M_{\eta_s} = M_{\phi} = \begin{pmatrix} 0 & 0 & 0 \\ 0 & 0 & 0 \\ 0 & 0 & 1 \end{pmatrix},$$

$$M_{\pi^-} = M_{\rho^-} = M_{\pi^+}^T, \qquad M_{K^-} = M_{K^{*-}} = M_{K^+}^T,$$
$$M_{\bar{K}^0} = M_{\bar{K}^{*0}} = M_{K^0}^T. \tag{A1}$$

We also need the following matrices:

$$\delta_u = \begin{pmatrix} 1 & 0 & 0 \\ 0 & 0 & 0 \\ 0 & 0 & 0 \end{pmatrix}, \qquad \Lambda^d = \begin{pmatrix} 0 \\ 1 \\ 0 \end{pmatrix}, \qquad \Lambda^s = \begin{pmatrix} 0 \\ 0 \\ 1 \end{pmatrix}. \tag{A2}$$

Using the meson matrices, one can write the hard kernels appearing in $B \to M_1 M_2$ decays as

$$\begin{aligned}
T_1 &= c_1^f B M_2 \delta_u M_1 \Lambda^f + (c_2^f \pm c_3^f) B M_2 \Lambda^f \,\mathrm{Tr}[\delta_u M_1] \\
&\quad + c_4^f B M_2 M_1 \Lambda^f + (c_5^f \pm c_6^f) B M_2 \Lambda^f \,\mathrm{Tr}[M_1], \\
T_{1g} &= c_1^f B \delta_u M_1 \Lambda^f \,\mathrm{Tr}[M_2] + (c_2^f \pm c_3^f) B \Lambda^f \,\mathrm{Tr}[\delta_u M_1] \\
&\quad \times \mathrm{Tr}[M_2] + c_4^f B M_1 \Lambda^f \,\mathrm{Tr}[M_2] \\
&\quad + (c_5^f \pm c_6^f) B \Lambda^f \,\mathrm{Tr}[M_1]\,\mathrm{Tr}[M_2], \\
T_1^g &= c_g^f B M_2 \Lambda^f \,\mathrm{Tr}[M_1], \\
T_{1g}^g &= c_g^f B \Lambda^f \,\mathrm{Tr}[M_1]\,\mathrm{Tr}[M_2], \\
T_{1J} &= T_1(c_i^f \to b_i^f), \qquad T_{1Jg} = T_{1J}(c_i^f \to b_i^f), \\
T_{1J}^g &= T_1^g(c_i^f \to b_i^f), \qquad T_{1Jg}^g = T_{1g}^g(c_i^f \to b_i^f).
\end{aligned} \tag{A3}$$

If the emitted meson M_2 is a pseudoscalar, $c_2^f - c_3^f$ and $c_5^f - c_6^f$ in T_i are used. But for vector meson emission, we use plus signs in the combinations.

Using meson matrices, the charming penguins responsible for $B \to M_1 M_2$ decays can be determined in the same way. If the charming penguins in $B \to PP$ decays are considered, the master equation is

$$A_{cc}^{M_1 M_2} = B M_2 M_1 \Lambda^f A_{cc}^{PP} + B M_1 \Lambda^f \,\mathrm{Tr}[M_2] A_{ccg}^{PP}, \tag{A4}$$

where the A_{ccg} term is only responsible for the isosinglet mesons η_q and η_s. In $B \to VP$ decays, the charming penguins are

$$\begin{aligned}
A_{cc}^{M_1 M_2} &= B M_2 M_1 \Lambda^f A_{cc}^{VP} + B M_1 M_2 \Lambda^f A_{cc}^{PV} \\
&\quad + B M_1 \Lambda^f \,\mathrm{Tr}[M_2] A_{ccg}^{VP},
\end{aligned} \tag{A5}$$

where we take M_1 as a vector meson and M_2 as a pseudoscalar meson.

The master equations for hard kernels for chirally enhanced penguins are given by

$$\begin{aligned}
T_1^\chi &= c_{1(qfq)}^{1\chi} B M_2 M_1 \Lambda^f + c_{2(qfq)}^{1\chi} B M_2 Q M_1 \Lambda^f, \\
T_{1g}^\chi &= c_{1(qfq)}^{1\chi} B M_1 \Lambda^f \,\mathrm{Tr}[M_2] + c_{2(qfq)}^{1\chi} B Q M_1 \Lambda^f \,\mathrm{Tr}[M_2], \\
T_{1J}^\chi &= T_1^\chi(c_{1(qfq)}^{1\chi} \to c_{3(qfq)}^{2\chi}, c_{2(qfq)}^{1\chi} \to c_{4(qfq)}^{2\chi}), \\
T_{1Jg}^\chi &= T_{1g}^\chi(c_{1(qfq)}^{1\chi} \to c_{3(qfq)}^{2\chi}, c_{2(qfq)}^{1\chi} \to c_{4(qfq)}^{2\chi}).
\end{aligned} \tag{A6}$$

[1] M. Wirbel, B. Stech, and M. Bauer, Z. Phys. C **29**, 637 (1985).
[2] M. Bauer, B. Stech, and M. Wirbel, Z. Phys. C **34**, 103 (1987).
[3] A. Ali and C. Greub, Phys. Rev. D **57**, 2996 (1998).
[4] G. Kramer, W. F. Palmer, and H. Simma, Nucl. Phys. **B428**, 77 (1994).
[5] A. Ali, G. Kramer, and C. D. Lu, Phys. Rev. D **58**, 094009 (1998).
[6] A. Ali, G. Kramer, and C. D. Lu, Phys. Rev. D **59**, 014005 (1998).
[7] Y. H. Chen, H. Y. Cheng, B. Tseng, and K. C. Yang, Phys. Rev. D **60**, 094014 (1999).
[8] M. Beneke, G. Buchalla, M. Neubert, and C. T. Sachrajda, Phys. Rev. Lett. **83**, 1914 (1999).
[9] M. Beneke, G. Buchalla, M. Neubert, and C. T. Sachrajda,

Nucl. Phys. **B591**, 313 (2000).
[10] M. Beneke and M. Neubert, Nucl. Phys. **B675**, 333 (2003).
[11] Y. Y. Keum, H. n. Li, and A. I. Sanda, Phys. Lett. B **504**, 6 (2001).
[12] Y. Y. Keum, H. N. Li, and A. I. Sanda, Phys. Rev. D **63**, 054008 (2001).
[13] C. D. Lu, K. Ukai, and M. Z. Yang, Phys. Rev. D **63**, 074009 (2001).
[14] C. W. Bauer, S. Fleming, D. Pirjol, and I. W. Stewart, Phys. Rev. D **63**, 114020 (2001).
[15] C. W. Bauer, D. Pirjol, and I. W. Stewart, Phys. Rev. Lett. **87**, 201806 (2001).
[16] C. W. Bauer, D. Pirjol, and I. W. Stewart, Phys. Rev. D **65**, 054022 (2002).
[17] C. W. Bauer, S. Fleming, D. Pirjol, I. Z. Rothstein, and I. W. Stewart, Phys. Rev. D **66**, 014017 (2002).
[18] J. Chay and C. Kim, Phys. Rev. D **68**, 071502 (2003).
[19] J. Chay and C. Kim, Nucl. Phys. **B680**, 302 (2004).
[20] C. W. Bauer, D. Pirjol, I. Z. Rothstein, and I. W. Stewart, Phys. Rev. D **70**, 054015 (2004).
[21] M. Beneke and S. Jager, Nucl. Phys. **B751**, 160 (2006).
[22] M. Beneke and S. Jager, Nucl. Phys. **B768**, 51 (2007).
[23] A. Jain, I. Z. Rothstein, and I. W. Stewart, arXiv:0706.3399.
[24] C. M. Arnesen, Z. Ligeti, I. Z. Rothstein, and I. W. Stewart, Phys. Rev. D **77**, 054006 (2008).
[25] C. W. Bauer, I. Z. Rothstein, and I. W. Stewart, Phys. Rev. D **74**, 034010 (2006).
[26] C. W. Bauer, D. Pirjol, I. Z. Rothstein, and I. W. Stewart, Phys. Rev. D **72**, 098502 (2005).
[27] P. Colangelo, G. Nardulli, N. Paver, and Riazuddin, Z. Phys. C **45**, 575 (1990).
[28] M. Ciuchini, E. Franco, G. Martinelli, and L. Silvestrini, Nucl. Phys. **B501**, 271 (1997).
[29] M. Ciuchini, E. Franco, G. Martinelli, M. Pierini, and L. Silvestrini, Phys. Lett. B **515**, 33 (2001).
[30] A. R. Williamson and J. Zupan, Phys. Rev. D **74**, 014003 (2006); **74**, 039901(E)(2006).
[31] For a review, see G. Buchalla, A. J. Buras, and M. E. Lautenbacher, Rev. Mod. Phys. **68**, 1125 (1996).
[32] M. Beneke, A. P. Chapovsky, M. Diehl, and T. Feldmann, Nucl. Phys. **B643**, 431 (2002).
[33] T. Feldmann, P. Kroll, and B. Stech, Phys. Rev. D **58**, 114006 (1998).
[34] T. Feldmann, P. Kroll, and B. Stech, Phys. Lett. B **449**, 339 (1999).
[35] T. Feldmann, Int. J. Mod. Phys. A **15**, 159 (2000).
[36] A. Hardmeier, E. Lunghi, D. Pirjol, and D. Wyler, Nucl. Phys. **B682**, 150 (2004).
[37] J. Charles *et al.* (CKMfitter Group), Eur. Phys. J. C **41**, 1 (2005). The updated results can be found at http://ckmfitter.in2p3.fr/.
[38] P. Ball and G. W. Jones, J. High Energy Phys. 03 (2007) 069.
[39] E. Barberio *et al.* (Heavy Flavor Averaging Group), arXiv: hep-ex/0603003. The updated results can be found at http://www.slact.stanford.edu/xorg/hfag.
[40] W. M. Yao *et al.* (Particle Data Group), J. Phys. G **33**, 1 (2006).
[41] C. D. Lu and M. Z. Yang, Eur. Phys. J. C **23**, 275 (2002).
[42] X. Liu, H. Wang, Z. Xiao, L. Guo, and C. D. Lu, Phys. Rev. D **73**, 074002 (2006).
[43] L. Guo, Q.-g. Xu, and Z.-j. Xiao, Phys. Rev. D **75**, 014019 (2007).
[44] D. Q. Guo, X. F. Chen, and Z.-j. Xiao, Phys. Rev. D **75**, 054033 (2007).
[45] A. Höcker, M. Laget, S. Laplace, and J.-v. Wimmersperg-Toeller, Report No. LAL 03-17.
[46] H.-n. Li, S. Mishima, and A. I. Sanda, Phys. Rev. D **72**, 114005 (2005).
[47] A. G. Akeroyd, C. H. Chen, and C. Q. Geng, Phys. Rev. D **75**, 054003 (2007).
[48] A. Ali *et al.*, Phys. Rev. D **76**, 074018 (2007).
[49] D. Du, H. Gong, J. Sun, D. Yang, and G. Zhu, Phys. Rev. D **65**, 094025 (2002); **66**, 079904(E) (2002).
[50] D. Du, J. Sun, D. Yang, and G. Zhu, Phys. Rev. D **67**, 014023 (2003).
[51] J. Sun, G. Zhu, and D. Du, Phys. Rev. D **68**, 054003 (2003).
[52] B. Dutta, C. S. Kim, S. Oh, and G. Zhu, Phys. Lett. B **601**, 144 (2004).
[53] X. Li and Y. Yang, Phys. Rev. D **73**, 114027 (2006).
[54] C. H. Chen, Y.-Y. Keum, and H.-n. Li, Phys. Rev. D **64**, 112002 (2001).
[55] C. H. Chen, Phys. Lett. B **525**, 56 (2002).
[56] Y.-Y. Keum, arXiv:hep-ph/0210127.
[57] S. Mishima and A. I. Sanda, Prog. Theor. Phys. **110**, 549 (2003).
[58] Z. Xiao, X. Chen, and D. Guo, Eur. Phys. J. C **50**, 363 (2007).
[59] X. Chen, D. Guo, and Z. Xiao, arXiv:hep-ph/0701146.
[60] Y.-Y. Charng, T. Kurimoto, and H.-n. Li, Phys. Rev. D **74**, 074024 (2006).
[61] M. Beneke, G. Buchalla, C. Greub, A. Lenz, and U. Nierste, Phys. Lett. B **459**, 631 (1999); A. Lenz and U. Nierste, J. High Energy Phys. 06 (2007) 072.
[62] M. Gronau, Phys. Lett. B **492**, 297 (2000).
[63] H. J. Lipkin, Phys. Lett. B **621**, 126 (2005).
[64] H.-n. Li and S. Mishima, Phys. Rev. D **73**, 114014 (2006).
[65] H.-n. Li and S. Mishima, Phys. Rev. D **74**, 094020 (2006).
[66] S. Nandi and H.-n. Li, Phys. Rev. D **76**, 034008 (2007).
[67] H. Tao and X.-G. Wu, Phys. Rev. D **71**, 034018 (2005).
[68] X.-G. Wu, T. Huang, and Z.-Y. Fang, Eur. Phys. J. C **52**, 561 (2007).
[69] B. H. Hong and C. D. Lu, Sci. China G **49**, 357 (2006).
[70] H.-n. Li, Phys. Lett. B **622**, 63 (2005).
[71] M. Beneke, G. Buchalla, M. Neubert, and C. T. Sachrajda, Phys. Rev. D **72**, 098501 (2005).
[72] H.-Y. Cheng, C.-K. Chua, and A. Soni, Phys. Rev. D **71**, 014030 (2005).
[73] C.-D. Lu, Y.-L. Shen, and W. Wang, Phys. Rev. D **73**, 034005 (2006).